

Current through a multi-lead junction caused by applied bias with arbitrary time-dependence

Michael Ridley^{1,2}, Angus MacKinnon², Lev Kantorovich¹

June 1, 2022

¹Department of Physics, King's College London, Strand, London, WC2R 2LS, United Kingdom

²Department of Physics, The Blackett Laboratory, Imperial College London, South Kensington Campus, London SW7 2AZ, United Kingdom

Abstract

We apply the Nonequilibrium Green's Function (NEGF) formalism to the problem of a multi-terminal nanojunction subject to an arbitrary time-dependent bias. In particular, we show that taking a generic one-particle system Hamiltonian within the wide band limit approximation (WBLA), it is possible to obtain a closed analytical expression for the current in each lead. Our formula reduces to the well-known result of Jauho *et. al.* [doi:10.1103/PhysRevB.50.5528] in the limit where the switch-on time is taken to the remote past, and to the result of Tuovinen *et. al.* [doi:10.1088/1742-6596/427/1/012014] when the bias is maintained at a constant value after the switch-on. As we use a partition-free approach, our formula contains both the long-time current and transient effects due to the sudden switch-on of the bias. Numerical calculations performed for the simple case of a single-level quantum dot coupled to two leads are performed for a sinusoidally-varying bias. At certain frequencies of the driving bias, we observe 'ringing' oscillations of the current, whose dependence on the dot level, level width, oscillation amplitude and temperature is also investigated.

1 Introduction

The problem of computing the nonlinear current response to a bias dropped across a nanoscale structure can be treated within the framework of the Nonequilibrium Green's Function (NEGF) formalism[1, 2, 3, 4, 5, 6, 7, 8]. This is an exact method for the calculation of time-dependent ensemble averages in many-electron systems both in and out of equilibrium, which automatically preserves all required conservation laws[9, 8]. The mathematical equivalence of the Green's function approaches to the nonequilibrium and equilibrium problems has been well understood since the work of Martin, Schwinger, Matsubara, Keldysh, Kadanoff and Baym [2, 1, 5, 4]. Perhaps the most elegant depiction of this equivalence comes with the introduction of the Konstantinov-Perel' contour, on which the initial preparation of the system together with its subsequent time evolution can be conveniently represented[3, 5].

In this paper, we are concerned with the problem of electron transport through a nanojunction, consisting of a small central region C , contacted with a set of conducting leads labelled by α , themselves in contact with an external circuit and battery. This may for example describe a molecule or quantum dot contacted with a pair of capacitor plates, as found for example in a single electron transistor[10]; a schematic of the generic set-up is shown in Fig. 1.

For noninteracting systems the Landauer-Büttiker (LB) formalism has enjoyed great success as a tool for the description of transport processes in the steady-state regime, when a long time has passed after the switch on of a constant bias [11, 12, 13, 14, 15]. This success may be attributed to its formal and conceptual simplicity, and a set of equations for the steady-state current that can be combined with DFT calculations to access the electronic properties of a system[16]. It is useful for the description of transport processes in the ballistic regime, where the time separating electron-electron interaction events exceeds the time taken for an electron to cross the molecular region. The LB formalism is convenient for the description of several features of transport processes accessible to experimentalists: temperature-dependence[17], quantization of the conductance[18, 19], exponential decay of conductance as a function of junction length[19, 20], and the shot and thermal noise associated with the current[14, 21].

In recent years, experimental work has increasingly focused on dynamical properties of nanojunctions, in particular the AC current response to a periodic voltage operating in the GHz or THz frequency range[22, 23, 24]. It is therefore desirable to develop a formalism that will allow calculation of the full time-dependent response of a molecular device to an arbitrary time-dependent perturbation.

Various approaches for going beyond the steady-state exist. Neglecting interactions, these tend to involve extensions of the LB formalism to time-dependent systems (TD-LB). In particular, recent progress has been made by the construction of explicit scattering state solutions for electrons incident on time-periodic non-stationary scatterers[25].

The understanding of transport processes are fundamentally problems in nonequilibrium statistical mechanics, because they typically involve a sudden 'switch-on' of a coupling between subsystems or a bias across subsystems which breaks the physical symmetry between the system at $t = -\infty$ and $t = +\infty$. This means that if the system was prepared in an equilibrium state in the distant past, it will not relax back to its initial state in the far future. Historically, there have been two main approaches to this kind of switch-on problem. In *partitioned* approaches[26, 27, 28, 29, 30] the system consists initially of decoupled leads with different chemical potentials μ_α . At the initial time t_0 , an idealized coupling between C and the leads is added to the Hamiltonian. The presence of the coupling enables electrons to hop between the $\alpha - C$ regions in the direction of decreasing chemical potential, and the LB formula is derived as the long-time limit of the resulting electron current. This means that the appropriate electronic couplings are not present in the equilibrium Hamiltonian prior to the switch-on, and that embedding self-energies cannot be defined for the system in equilibrium. However, this is not important for deriving the steady state expression for the current as it is assumed that at long times all preparation-dependent effects have been washed out. Working within a partitioned approach, Jauho et. al. obtained a closed (ω, t) -space integral expression for the TD current response to an arbitrary time varying bias[28, 29]. They assumed that the decoupled leads were prepared at $t_0 = -\infty$ with an appropriate time dependent bias and then, immediately after, the coupling between the leads and the central system was enabled. Naturally, this approach has a problem as the bias and the coupling are being established at the same time in the distant past. Therefore, the correctness of this approach rests on an assumption that the system arrives at the correct non-equilibrium state at times $t > 0$ after a semi-infinite development from $-\infty$, which cannot be guaranteed as the perturbation due to the coupling *and* the bias were added together. Also, in terms of applications, the partitioned approach is limited to a periodic bias only; for instance, the 'switch on' effect can only be modelled by considering periodic bias pulses well separated in time. However, a finite time between pulses prevents the system from equilibrating properly. However, in a real experiment, one switches on the bias, not the coupling between regions. The coupling will be fully present at equilibrium, so that a single inverse temperature β and single chemical potential μ are defined for all regions of the junction. *Partition-free* approaches[31, 32, 33] recognise this fact, and therefore they effectively diverge from partitioned approaches in their choice of initial density matrix ρ_0 for the many-body dynamics. After t_0 , the same Hamiltonian is used to propagate the system in either of the two approaches, so if all information on the preparation of the system is lost in the long-time limit, one would expect the same steady state to be reached regardless of the choice of the initial density matrix.

However, whereas the equilibrium initial distribution in the partition-free approach is well-defined and leads to a physical transient current, any transients in the partitioned approach cannot be interpreted physically, as they result from the junction's 'memory' of its fictitious initial state. Important progress was made in the direction of a fully time-dependent partition-free approach by Stefanucci and Almladh, who proved theorems of asymptotic equivalence between the two approaches and obtained an integral formula for the linear current response to a TD bias within the Wide-Band-Limit Approximation (WBLA)[32]. Recently, Tuovinen *et. al.* obtained a closed frequency integral for the exact time-dependent current response to a static bias, within a partition-free approach, making it increasingly possible to theoretically investigate short-time effects in nanoscale systems[8, 34]. Their formula clearly exhibits decaying modes in addition to a steady-state part, and has been applied to the study of transport through ring-shaped molecular junctions[34], and more recently, graphene nanoribbons[33].

Here we develop an analytic approach whereby a TD-LB formula for a current response to an *arbitrary* time-dependent bias in a multi-lead system, including the 'switch-on' effect, is derived, for any tight-binding Hamiltonian. The final formula involves only slightly more computational cost than the corresponding LB formula for the steady-state current. In our formulation we extend the partition-free approach of [34, 8], in that no assumptions are made concerning the particular time dependence of the bias applied to each of the leads. The analytical result is obtained within the WBLA by integrating exactly the Kadanoff-Baym equations for the Green's function of the central region. This work incorporates the formulae of Jauho et. al. and Tuovinen et. al. as special cases. Specifically, the former emerges as the long time limit of a more general expression that contains the transients. The latter is the constant bias limit of our more general expression containing time integrals of the bias. In this way we show that an analytical expression for the fully non-linear current response to an arbitrary TD bias at all times subsequent to t_0 is possible within the WBLA.

Note in passing that a numerical approach to the solution of the embedded Kadanoff-Baym equations for systems that include an explicit electron-electron interaction term in their Hamiltonian within the Second Born (2B) and GW approximations has also been recently developed[35, 36, 37, 33]. Extensions of the tight-binding approach to a DFT-Green's function formalism in the time domain have also been performed. In these approaches, the system is prepared in an equilibrium state whose electronic structure is obtained from *ab initio* calculations, before the time-dependent perturbation is applied[38]. We do not take these approaches here as they can only be facilitated numerically. We believe that a great deal of physics is readily accessible with a simple tight-binding model and a simplified treatment of the coupling (the essence of the WBLA). Some physical effects that one would expect to observe, for example in the case of a periodic bias, include asymmetry of the current signal about the voltage peak, and a quickly oscillating transient, the so-called 'ringing' of the current immediately after the switch-on. In the NEGF-based formalism for calculating the current response to an arbitrary time-dependent bias these effects are clearly observable, amongst others. We emphasize that our formalism is not limited to the case of a periodic bias, and therefore offers an alternative to the non-stationary

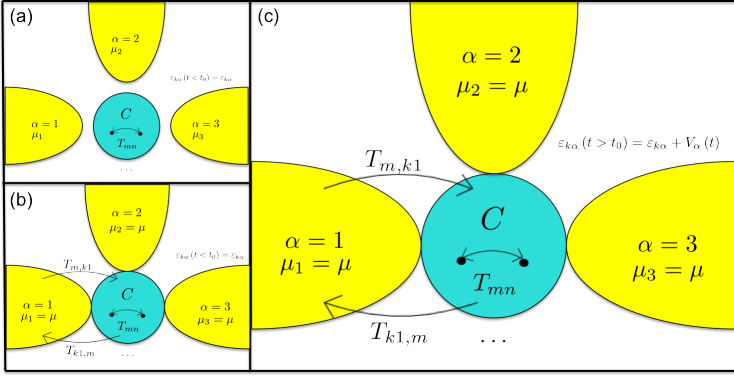


Figure 1: Schematic of the multi-terminal nanojunction in the time regimes before and after t_0 : (a) $t < t_0$ in the partitioned approach; (b) $t < t_0$ in the partition-free approach; (c) $t \geq t_0$ in either approach.

S-matrix approaches which rely on the Floquet theorem.

The paper is organised as follows: section 2 contains a description of the model Hamiltonian, the derivation of self-energies and all components of the Green's functions required for the current. In particular, a novel formula for the exact lesser Green's function of two times is presented here. From this, an (ω, t) integral is derived for the current through one of the leads, and we proceed to show how it reduces to known results in the long-time and static bias limits. Note that some steps of our calculation are similar to those done in [34]. In these cases we do not give much detail; instead we briefly outline a few essential steps and state the final results. In Section 3 we present the results of current calculations on a quantum dot central region in response to a periodic external bias. Appendices A to C contain details of the calculation of the lesser Green's function and of the current.

2 Theory

2.1 Hamiltonian on the contour

The Kadanoff-Baym or Nonequilibrium Green's function (NEGF) approach to electron transport is a tool for the description of the time evolution ensemble averages of quantum systems; in particular, it can conveniently be used for calculating time dependent ensemble averages of particle number densities in subsystems open to an environment.

The most essential feature of this formalism is that of time evolution on a contour defined in the complex time plane. Here, γ refers to the Konstantinov-Perel' contour, which is just the union of the three sets of points: (i) C_- , the 'upper' contour, containing points between $t_0 + i0$ and $t + i0$; (ii) the lower' contour C_+ containing points along the line between $t - i0$ and $t_0 - i0$, and (iii) C_M which is any contour in the complex plane between two points z_a, z_b , such that $z_b - z_a = -i\beta$, where $\beta = 1/k_B T$ is the inverse temperature. Usually one chooses $z_a = t_0 - i0$ and $z_b = t_0 - i\beta$, and connects them with a vertical path on the contour as shown in Fig. 2. At 'times' that lie on C_M the system exists in thermodynamic equilibrium since this part of the contour originates from the initial density operator $\hat{\rho}_0 = Z^{-1} e^{-\beta(\hat{H}_0 - \mu\hat{N})}$, with μ being the chemical potential of the whole system and \hat{N} the particle number operator. The times on the contour are ordered from $t_0 + i0$ to $t_0 - i\beta$ and then to $t - i\beta$ as shown by the arrows in 2. In this paper we use the units in which $\hbar = 1$.

The variable z will be used to indicate the 'time' along the contour, and the system Hamiltonian $\hat{H}(z)$ must be specified for all z . When used between z -variables, the symbols ' $>$ ' / ' $<$ ' mean 'later/earlier on the contour', where z_1 is later than z_2 on the contour if a directed line drawn from the point t_{0-} to $t_0 - i\beta$ passes through z_2 before passing through z_1 . In general, the definition of the Hamiltonian will be different on different parts of the contour, containing both equilibrium and nonequilibrium parts; for instance, the non-equilibrium part contains the bias which is missing in \hat{H}_0 defined on the vertical track. For the typical set-up of a quantum transport problem, we therefore have the following Hamiltonian:

$$\hat{H}(z) = \sum_{k\alpha\sigma} \varepsilon_{k\alpha}(z) \hat{d}_{k\alpha\sigma}^\dagger \hat{d}_{k\alpha\sigma} + \sum_{mn\sigma} T_{mn}(z) \hat{d}_{m\sigma}^\dagger \hat{d}_{n\sigma} + \sum_{m,k\alpha\sigma} \left[T_{m,k\alpha}(z) \hat{d}_{m\sigma}^\dagger \hat{d}_{k\alpha\sigma} + T_{k\alpha,m}(z) \hat{d}_{k\alpha\sigma}^\dagger \hat{d}_{m\sigma} \right] \quad (1)$$

The first term in this expression corresponds to the sum of the Hamiltonians of the reservoirs/leads, where α labels the lead, and k labels the k -th eigenstate of this lead. The second term corresponds to the Hamiltonian of the central region C and hence refers to electron hopping events within this region with indices n and m labeling eigenstates there. Finally, the third term describes the coupling of the leads and the central system with the corresponding matrix elements $T_{m,k\alpha}$, and σ denotes the spin degree of freedom of the electrons. Correspondingly, $\hat{d}_{k\alpha\sigma}$, $\hat{d}_{m\sigma}$ and $\hat{d}_{k\alpha\sigma}^\dagger$, $\hat{d}_{m\sigma}^\dagger$ are destruction and creation operators of the leads and the central system.

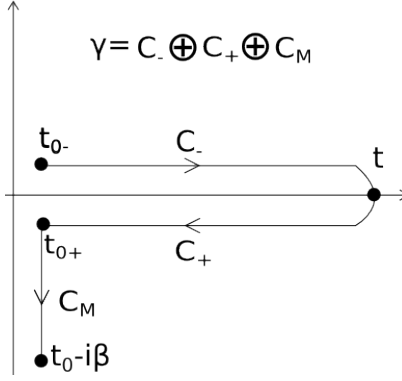


Figure 2: The Konstantinov-Perel' Contour $\gamma \equiv C_- \oplus C_+ \oplus C_M$.

In the following, bold letters will be used for matrices. We shall omit the spin index for simplicity of notation; it can be trivially introduced back in the final results if desired. It is useful at this point to introduce a matrix $\mathbf{h}(z)$, defined on the basis of the whole multi-terminal system, so that the Hamiltonian (1) can be rewritten simply as

$$\hat{H}(z) = \sum_{ij} h_{ij} \hat{d}_i^\dagger \hat{d}_j \quad (2)$$

where we sum over all orbitals i, j of the leads and the central system, h_{ij} are elements of the matrix \mathbf{h} , and d_i, d_i^\dagger correspond to the operators of either the leads (if $i \equiv k\alpha$) or C (if $i \equiv n$). It is also convenient to introduce blocks of the matrix \mathbf{h} , projected onto the molecule or reservoir subspaces, i.e. $\mathbf{h}_{\alpha\alpha'}(z)$ is the block of $\mathbf{h}(z)$ with matrix elements $[\mathbf{h}_{\alpha\alpha'}]_{kk'} = \delta_{\alpha\alpha'} \delta_{kk'} \varepsilon_{k\alpha}(z)$ (note that there is no interaction between leads, so that $\mathbf{h}_{\alpha\alpha'} = \delta_{\alpha\alpha'} \mathbf{h}_{\alpha\alpha}$), $\mathbf{h}_{\alpha C}$ is the block of $\mathbf{h}(z)$ with matrix elements $[\mathbf{h}_{\alpha C}]_{km} = T_{k\alpha, m}(z)$, and \mathbf{h}_{CC} is the block of $\mathbf{h}(z)$ with matrix elements $[\mathbf{h}_{CC}]_{mn} = T_{mn}(z)$. We assume that prior to the switch on at time t_0 the whole electron system was in thermodynamic equilibrium characterised by the unique chemical potential μ and inverse temperature β . Then at t_0 each lead α is subjected to the arbitrary bias potential $V_\alpha(t)$. Then on different parts of the contour γ the elements of the matrix $\mathbf{h}(z)$ are defined as follows:

$$[\mathbf{h}_{\alpha\alpha}(z)]_{kk'} = \begin{cases} (\varepsilon_{k\alpha} + V_\alpha(t)) \delta_{kk'}, & z \equiv t \in C_- \oplus C_+ \\ (\varepsilon_{k\alpha} - \mu) \delta_{kk'}, & z \in C_M \end{cases} \quad (3)$$

$$[\mathbf{h}_{C\alpha}(z)]_{mk} = T_{mk, \alpha}, \quad z \in \gamma \quad (4)$$

$$[\mathbf{h}_{CC}(z)]_{mn} = \begin{cases} T_{mn}, & z \in C_- \oplus C_+ \\ T_{mn} - \mu \delta_{mn}, & z \in C_M \end{cases} \quad (5)$$

This Hamiltonian corresponds to the switch-on of a spatially uniform bias in each reservoir.

One note is in order here. The experimentalist in such systems typically has control over the voltage passed across the nanojunction. At some initial time t_0 , the switch-on of a bias means that energy levels in lead α are shifted by some external bias, $V_\alpha(t)$. In general, an external field will cause a rearrangement of electrons in the junction and leads. In particular, the electrons in the conducting leads will screen the external field so that the electric field inside the conductor equals zero and its electric potential is uniform throughout. This leads to confinement of the drop in potential to the region C , and means that $V_\alpha(t)$ should not be interpreted as $eV(t)$, where $V(t)$ is the actual voltage across the whole macroscopic lead. Rather, it should be equal to the sum of $eV(t)$ and the screening potential induced by the switch-on. However, the central region C can always be chosen sufficiently large that a part of each lead neighbouring C , which is mostly affected by the charge redistribution is incorporated into C . In this case we may assume that the potential $V_\alpha(t)$ is uniform across the lead α and is equal to the bias voltage applied to this particular lead.

2.2 Greens function components

The one-particle Green's function on the contour γ is defined in the usual way as:

$$G_{ij}(z_1, z_2) \equiv -i \frac{\text{Tr} \left\{ e^{-\beta \hat{H}_M} \hat{T}_\gamma \left[\hat{d}_{H,i}(z_1) \hat{d}_{H,j}^\dagger(z_2) \right] \right\}}{\text{Tr} \left(e^{-\beta \hat{H}_M} \right)}$$

where \hat{T}_γ is the 'time' ordering operator on the contour γ , \hat{H}_M is the Hamiltonian on its vertical part, and the subscript H by the creation and annihilation operators means that these are considered in the Heisenberg picture on the contour. The

elements G_{ij} of the Green's function form a matrix \mathbf{G} defined on the whole space of orbitals of all leads and the central region; correspondingly, one can introduce diagonal, \mathbf{G}_{CC} and $\mathbf{G}_{\alpha\alpha}$, as well as non-diagonal, $\mathbf{G}_{C\alpha}$ and $\mathbf{G}_{\alpha C}$, blocks of this matrix. The Green's function \mathbf{G}_{CC} for the central region satisfies the equations of motion:

$$\left[i \frac{d}{dz_1} - \mathbf{h}_{CC}(z_1) \right] \mathbf{G}_{CC}(z_1, z_2) = \mathbf{1}_{CC} \delta(z_1, z_2) + \int_{\gamma} d\bar{z} \mathbf{\Sigma}_{CC}(z_1, \bar{z}) \mathbf{G}_{CC}(\bar{z}, z_2) \quad (6)$$

$$\mathbf{G}_{CC}(z_1, z_2) \left[-i \frac{\overleftarrow{d}}{dz_2} - \mathbf{h}_{CC}(z_2) \right] = \mathbf{1}_{CC} \delta(z_1, z_2) + \int_{\gamma} d\bar{z} \mathbf{G}_{CC}(z_1, \bar{z}) \mathbf{\Sigma}_{CC}(\bar{z}, z_2) \quad (7)$$

where $\mathbf{1}_{CC}$ is the unit matrix defined on the orbitals of C , and

$$\mathbf{\Sigma}_{CC}(z_1, z_2) = \sum_{\alpha} \mathbf{h}_{C\alpha}(z_1) \mathbf{g}_{\alpha\alpha}(z_1, z_2) \mathbf{h}_{\alpha C}(z_2) \quad (8)$$

is the matrix of the embedded self-energy, while the non-diagonal matrix blocks of the Green's function are given by the integrals on the contour:

$$\mathbf{G}_{\alpha C}(z_1, z_2) = \int_{\gamma} d\bar{z} \mathbf{g}_{\alpha\alpha}(z_1, \bar{z}) \mathbf{h}_{\alpha C}(\bar{z}) \mathbf{G}_{CC}(\bar{z}, z_2) \quad (9)$$

$$\mathbf{G}_{C\alpha}(z_1, z_2) = \int_{\gamma} d\bar{z} \mathbf{G}_{CC}(z_1, \bar{z}) \mathbf{h}_{C\alpha}(\bar{z}) \mathbf{g}_{\alpha\alpha}(\bar{z}, z_2) \quad (10)$$

Here $\mathbf{g}_{\alpha\alpha}(z_1, z_2)$ is the Green's function of an isolated lead α corresponding to the Hamiltonian with the matrix block $\mathbf{h}_{\alpha\alpha}(z)$; note that the latter contains the term with the bias.

Depending on the positions of the 'time' arguments z_1 and z_2 on γ , special notations are normally used for the Green's functions defining its various components: if z_1, z_2 belong to either of the horizontal parts of γ with $z_1 > z_2$ or $z_1 < z_2$, then the greater, $\mathbf{G}^>(t_1, t_2)$, or lesser, $\mathbf{G}^<(t_1, t_2)$, components are defined, respectively; if one of the times lies on the vertical part and another on a horizontal one, then the right, $\mathbf{G}^{\Gamma}(t_1, \tau_2)$, and left, $\mathbf{G}^{\Gamma}(t_1, \tau_2)$, components are introduced, respectively, where t_1 or t_2 lie on the horizontal parts while another arguments τ_1 or τ_2 correspond to the 'times' $t_0 - i\tau_1$ or $t_0 - i\tau_2$ on the vertical part of γ ; finally, it is also convenient to consider the case when both times lie on the vertical part of γ in which case $\mathbf{G}(z_1, z_2)$ coincides with the Matsubara Green's function $\mathbf{G}^M(\tau_1, \tau_2)$. In addition to the objects defined above, on the horizontal part of γ we define, respectively, the retarded and advanced Green's functions:

$$\begin{aligned} \mathbf{G}^r(t_1, t_2) &= \theta(t_1 - t_2) [\mathbf{G}^>(t_1, t_2) - \mathbf{G}^<(t_1, t_2)] \\ \mathbf{G}^a(t_1, t_2) &= -\theta(t_2 - t_1) [\mathbf{G}^>(t_1, t_2) - \mathbf{G}^<(t_1, t_2)] \end{aligned}$$

where $\theta(t)$ is the unit step function.

2.3 Self-energies in the WBLA

Depending on where the two 'time' arguments in the self-energy $\mathbf{\Sigma}_{CC}(z_1, z_2)$ lie, various components of it can also be defined. These require calculation of the corresponding components of the Green's function $\mathbf{g}_{\alpha\alpha}(z_1, z_2)$ of the isolated lead α . The time-dependent part, $\sum_k V_{\alpha}(t) \hat{N}_{k\alpha}$ (where $\hat{N}_{k\alpha} = \hat{d}_{k\alpha}^{\dagger} \hat{d}_{k\alpha}$ is the number operator), in the Hamiltonian of the lead α commutes with the rest of its Hamiltonian and hence the time ordering can be omitted when calculating the corresponding evolution operator. Hence, the expressions for the creating and annihilation operators in the Heisenberg representation follow immediately: if $z \equiv t \in C_{\pm}$, then

$$\hat{d}_{k\alpha}(t) = \hat{d}_{k\alpha} e^{-i\phi_{k\alpha}(t, t_0)} = \left[\hat{d}_{k\alpha}^{\dagger}(t) \right]^{\dagger}$$

where it is convenient to introduce a function

$$\phi_{k\alpha}(t, t_0) = (t - t_0) \epsilon_{k\alpha} + \int_{t_0}^t V_{\alpha}(\tau) d\tau = (t - t_0) \epsilon_{k\alpha} + \psi_{\alpha}(t, t_0);$$

if $z = t_0 - i\tau \in C_M$, then the creation/annihilation operators are no longer Hermitian conjugates of each other:

$$\begin{aligned} \hat{d}_{k\alpha}(t_0 - i\tau) &= \hat{d}_{k\alpha} e^{-(\epsilon_{k\alpha} - \mu)\tau} \\ \hat{d}_{k\alpha}^{\dagger}(t_0 - i\tau) &= \hat{d}_{k\alpha}^{\dagger} e^{(\epsilon_{k\alpha} - \mu)\tau} \end{aligned}$$

Using these operators and the definition of the Green's functions, different components of the lead Green's functions are obtained:

$$\begin{aligned} [\mathbf{g}_{\alpha\alpha}^T(t_1, t_2)]_{kk'} &= -i\theta(t_1 - t_2) \delta_{kk'} e^{-i\phi_{k\alpha}(t_1, t_2)} \\ [\mathbf{g}_{\alpha\alpha}^a(t_1, t_2)]_{kk'} &= i\theta(t_2 - t_1) \delta_{kk'} e^{-i\phi_{k\alpha}(t_1, t_2)} \\ [\mathbf{g}_{\alpha\alpha}^<(t_1, t_2)]_{kk'} &= i\delta_{kk'} f(\varepsilon_{k\alpha} - \mu) e^{-i\phi_{k\alpha}(t_1, t_2)} \\ [\mathbf{g}_{\alpha\alpha}^>(t_1, t_2)]_{kk'} &= -i\delta_{kk'} [1 - f(\varepsilon_{k\alpha} - \mu)] e^{-i\phi_{k\alpha}(t_1, t_2)} \end{aligned}$$

Here $f(\omega) = (e^{\beta\omega} + 1)^{-1}$ is the Fermi function. In the case of the Matsubara component, it is convenient to expand it into a Fourier series, which is possible due to the boundary conditions, $\mathbf{g}_{\alpha\alpha}^M(\tau, 0) = -\mathbf{g}_{\alpha\alpha}^M(\tau, \beta)$ and $\mathbf{g}_{\alpha\alpha}^M(0, \tau) = -\mathbf{g}_{\alpha\alpha}^M(\beta, \tau)$:

$$[\mathbf{g}_{\alpha\alpha}^M(\tau_1, \tau_2)]_{kk'} = \delta_{kk'} \frac{i}{\beta} \sum_q \frac{e^{-\omega_q(\tau_1 - \tau_2)}}{\omega_q - \varepsilon_{k\alpha} + \mu}$$

where $\omega_q = i\pi(2q + 1)/\beta$ are Matsubara frequencies and the q summation is run over all negative and positive integers. Then, the right and left components can also be written via the Matsubara sums:

$$\begin{aligned} [\mathbf{g}_{\alpha\alpha}^r(t, \tau)]_{kk'} &= [\mathbf{g}_{\alpha\alpha}^M(0, \tau)]_{kk'} e^{-i\phi_{k\alpha}(t, t_0)} = \delta_{kk'} \frac{i}{\beta} e^{-i\phi_{k\alpha}(t, t_0)} \sum_q \frac{e^{\omega_q \tau}}{\omega_q - \varepsilon_{k\alpha} + \mu} \\ [\mathbf{g}_{\alpha\alpha}^l(\tau, t)]_{kk'} &= [\mathbf{g}_{\alpha\alpha}^M(\tau, 0)]_{kk'} e^{i\phi_{k\alpha}(t, t_0)} = \delta_{kk'} \frac{i}{\beta} e^{i\phi_{k\alpha}(t, t_0)} \sum_q \frac{e^{-\omega_q \tau}}{\omega_q - \varepsilon_{k\alpha} + \mu} \end{aligned}$$

All the components of the self-energy can now be obtained from Eq. (8). To obtain the retarded component, we shall Fourier transform that part of the expression since it depends only on the time-difference $t_1 - t_2$:

$$\begin{aligned} [\Sigma_{CC}^r(t_1, t_2)]_{mn} &= \sum_{\alpha} e^{-i\psi_{\alpha}(t_1, t_2)} \int \frac{d\omega}{2\pi} e^{i\omega(t_1 - t_2)} \sum_k \frac{T_{m, k\alpha} T_{k\alpha, n}}{\omega + i0 - \varepsilon_{k\alpha}} \\ &= \sum_{\alpha} e^{-i\psi_{\alpha}(t_1, t_2)} \int \frac{d\omega}{2\pi} e^{i\omega(t_1 - t_2)} \left[\Lambda_{\alpha, mn}(\omega) - \frac{i}{2} \Gamma_{\alpha, mn}(\omega) \right] \end{aligned}$$

where (the symbol \mathcal{P} corresponds to the Cauchy principal part):

$$\begin{aligned} \Lambda_{\alpha, mn}(\omega) &= \mathcal{P} \int \frac{d\omega'}{2\pi} \frac{\Gamma_{\alpha, nm}(\omega')}{\omega - \omega'} \\ \Gamma_{\alpha, mn}(\omega) &= 2\pi \sum_k T_{m, k\alpha} T_{k\alpha, n} \delta(\omega - \varepsilon_{k\alpha}) \end{aligned}$$

In the WBLA it is assumed that the energy range of the transmission channel in the leads is so wide that the coupling between every lead state and a given molecular orbital is independent of the energy of the lead state; hence, the ω dependence of the level width matrix $\mathbf{\Gamma}_{\alpha} = \|\Gamma_{\alpha, mn}(\omega)\|$ is neglected, $\Gamma_{\alpha, mn}(\omega) \simeq \Gamma_{\alpha, mn}$, in which case the level shift matrix becomes exactly zero, $\Lambda_{\alpha}(\omega) = 0$. This is a good approximation in systems for which transport takes place at energies close to the Fermi level, and in cases where the matrices $\Lambda_{\alpha}(\omega)$ and $\mathbf{\Gamma}_{\alpha}(\omega)$ vary slowly with ω . This approximation finally gives a simple analytical result:

$$[\Sigma_{CC}^r(t_1, t_2)]_{mn} = -\frac{i}{2} \delta(t_1 - t_2) \Gamma_{mn} \quad (11)$$

where $\Gamma_{mn} = \sum_{\alpha} \Gamma_{\alpha, mn}$ is the total level width of the junction. Similarly,

$$[\Sigma_{CC}^a(t_1, t_2)]_{mn} = \frac{i}{2} \delta(t_1 - t_2) \Gamma_{mn} \quad (12)$$

In the WBLA, the lesser, greater, right and left self-energy components are obtained in a similar manner. We shall give them here for completeness:

$$[\Sigma_{CC}^<(t_1, t_2)]_{mn} = i \left[\sum_{\alpha} \Gamma_{\alpha, mn} e^{-i\psi_{\alpha}(t_1, t_2)} \right] \int \frac{d\omega}{2\pi} f(\omega - \mu) e^{-i\omega(t_1 - t_2)} \quad (13)$$

$$[\Sigma_{CC}^>(t_1, t_2)]_{mn} = -i \left[\sum_{\alpha} \Gamma_{\alpha, mn} e^{-i\psi_{\alpha}(t_1, t_2)} \right] \int \frac{d\omega}{2\pi} [1 - f(\omega - \mu)] e^{-i\omega(t_1 - t_2)} \quad (14)$$

$$[\Sigma_{CC}^r(\tau, t)]_{mn} = \frac{i}{\beta} \left[\sum_{\alpha} \Gamma_{\alpha, mn} e^{i\psi_{\alpha}(t, t_0)} \right] \sum_q e^{-\omega_q \tau} \int \frac{d\omega}{2\pi} \frac{e^{i\omega(t-t_0)}}{\omega_q - \omega + \mu} \quad (15)$$

$$[\Sigma_{CC}^l(t, \tau)]_{mn} = \frac{i}{\beta} \left[\sum_{\alpha} \Gamma_{\alpha, mn} e^{-i\psi_{\alpha}(t, t_0)} \right] \sum_q e^{\omega_q \tau} \int \frac{d\omega}{2\pi} \frac{e^{-i\omega(t-t_0)}}{\omega_q - \omega + \mu} \quad (16)$$

The Matsubara self-energy is obtained similarly with the help of the identity

$$\int \frac{d\omega}{2\pi} \frac{1}{\omega_q - \omega + \mu} = \frac{i}{2} \xi_q$$

Here $\xi_q = +1$ when $Im(\omega_q) > 0$ and $\xi_q = -1$ when $Im(\omega_q) < 0$. This finally gives:

$$[\Sigma_{CC}^M(\tau_1, \tau_2)]_{mn} = -\frac{\Gamma_{mn}}{2\beta} \sum_q \xi_q e^{-\omega_q(\tau_1 - \tau_2)} \quad (17)$$

One can see that expressions for the lesser, greater, right and left components of the self-energy differ from those obtained in [34, 8] for the case of the switched on constant bias; the expressions for the Matsubara, advanced and retarded components remain the same.

2.4 Integration of the Kadanoff-Baym equations

2.4.1 Matsubara Green's function

Projecting Eq. (6) on the vertical track of the contour γ and applying the Langreth rules[39, 6], the corresponding equation of motion for the Matsubara Green's function $\mathbf{G}_{CC}^M(\tau_1, \tau_2)$ is obtained:

$$\left[-\frac{d}{d\tau_1} - \mathbf{h}_{CC}^M \right] \mathbf{G}_{CC}^M(\tau_1, \tau_2) = i \mathbf{1}_{CC} \delta(\tau_1 - \tau_2) + (\Sigma_{CC}^M \star \mathbf{G}_{CC}^M)_{(\tau_1, \tau_2)} \quad (18)$$

where $\mathbf{h}_{CC}^M = \mathbf{h}_{CC} - \mu \mathbf{1}_{CC}$ is the Hamiltonian matrix of the central region on the vertical track of the contour γ with $(\mathbf{h}_{CC})_{mn} = T_{mn}$, while the star in the last term corresponds to the imaginary time convolution integral [8]:

$$(\Sigma_{CC}^M \star \mathbf{G}_{CC}^M)_{(\tau_1, \tau_2)} \equiv -i \int_0^{\beta} d\tau \Sigma_{CC}^M(\tau_1, \tau) \mathbf{G}_{CC}^M(\tau, \tau_2) \quad (19)$$

Expanding the self-energy $\Sigma_{CC}^M(\tau, \tau')$, the Green's function $\mathbf{G}_{CC}^M(\tau, \tau')$ and the delta function $\delta(\tau_1 - \tau_2)$ into the Matsubara sums, one immediately obtains:

$$\mathbf{G}_{CC}^M(\tau_1, \tau_2) = \frac{i}{\beta} \sum_q e^{-\omega_q(\tau_1 - \tau_2)} \begin{cases} [(\omega_q + \mu) \mathbf{1}_{CC} - \mathbf{h}_{CC}^{eff}]^{-1}, & Im(\omega_q) > 0 \\ [(\omega_q + \mu) \mathbf{1}_{CC} - (\mathbf{h}_{CC}^{eff})^{\dagger}]^{-1}, & Im(\omega_q) < 0 \end{cases} \quad (20)$$

$$\mathbf{G}_{CC}^M(\omega_q) = \begin{cases} [(\omega_q + \mu) \mathbf{1}_{CC} - \mathbf{h}_{CC}^{eff}]^{-1}, & Im(\omega_q) > 0 \\ [(\omega_q + \mu) \mathbf{1}_{CC} - (\mathbf{h}_{CC}^{eff})^{\dagger}]^{-1}, & Im(\omega_q) < 0 \end{cases} \quad (21)$$

where $\mathbf{h}_{CC}^{eff} = \mathbf{h}_{CC} - i\Gamma_{CC}/2$ is the ‘‘effective’’ Hamiltonian of region C . As expected, the Matsubara Green's function is the same as in [34]. This is to be expected as it corresponds to the preparation of the system prior to the switch on of the bias.

2.4.2 Right and left Green's functions

Projecting Eq. (6) on the right component (i.e. $t_1 \in C_- \oplus C_+$, $t_2 = t_0 - i\tau_2 \in C_M$) and using the Langreth rules again, the following equation of motion for the right Green's function is obtained:

$$\left(i \frac{d}{dt_1} - \mathbf{h}_{CC} \right) \mathbf{G}_{CC}^r(t_1, \tau_2) = (\Sigma_{CC}^r \cdot \mathbf{G}_{CC}^r + \Sigma_{CC}^r \star \mathbf{G}_{CC}^M)_{(t_1, \tau_2)}$$

where, following notations introduced in [8], we defined the dot-convolution (real time axis) integral

$$(\boldsymbol{\Sigma}_{CC}^r \cdot \mathbf{G}_{CC}^\top)_{(t,\tau)} = \int_{t_0}^{\infty} dt_1 \boldsymbol{\Sigma}_{CC}^r(t, t_1) \mathbf{G}_{CC}^\top(t_1, \tau) \quad (22)$$

Using expression for the retarded self-energy (11), the equation of motion is manipulated into:

$$\left(i \frac{d}{dt_1} - \mathbf{h}_{CC}^{eff} \right) \mathbf{G}_{CC}^\top(t_1, \tau_2) = (\boldsymbol{\Sigma}_{CC}^\top \star \mathbf{G}_{CC}^M)_{(t_1, \tau_2)}$$

which can be solved for the right Green's function taking into account the appropriate boundary conditions $\mathbf{G}_{CC}^\top(t_0, \tau) = \mathbf{G}_{CC}^M(0^-, \tau)$:

$$\mathbf{G}_{CC}^\top(t, \tau) = e^{-i\mathbf{h}_{CC}^{eff}(t-t_0)} \left[\mathbf{G}_{CC}^M(0^-, \tau) - i \int_{t_0}^t d\bar{t} e^{i\mathbf{h}_{CC}^{eff}(\bar{t}-t_0)} (\boldsymbol{\Sigma}_{CC}^\top \star \mathbf{G}_{CC}^M)_{(\bar{t}, \tau)} \right] \quad (23)$$

Similarly,

$$\mathbf{G}_{CC}^r(\tau, t) = \left[\mathbf{G}_{CC}^M(\tau, 0^-) + i \int_{t_0}^t d\bar{t} (\mathbf{G}_{CC}^M \star \boldsymbol{\Sigma}_{CC}^r)_{(\tau, \bar{t})} e^{-i(\mathbf{h}_{CC}^{eff})^\dagger(\bar{t}-t_0)} \right] e^{i(\mathbf{h}_{CC}^{eff})^\dagger(t-t_0)} \quad (24)$$

Note that the obtained expressions contain exponential functions of the matrix \mathbf{h}_{CC}^{eff} . Formally these expressions for the right and left Green's functions in terms of different components are identical to those given in [8] for the constant bias switch-on case. Note, however, that this apparent similarity is misleading as the detailed expressions for the right and left self-energies are not the same in the two cases.

2.4.3 Retarded and advanced Green's functions

It is well known that for the case of the static bias the retarded and advanced Green's functions of the whole system still depend on the time difference as in the stationary case. It is crucial for our derivation, in which the bias applied to each lead is time-dependent, that this property of these two Green's functions still holds. This can be shown by first projecting Eq. (6) on the retarded subspace of the (z_1, z_2) plane and applying the Langreth rules:

$$\left(i \frac{d}{dt_1} - \mathbf{h}_{CC} \right) \mathbf{G}_{CC}^r(t_1, t_2) = \mathbf{1}_{CC} \delta(t_1 - t_2) + (\boldsymbol{\Sigma}_{CC}^r \cdot \mathbf{G}_{CC}^r)_{(t_1, t_2)} \quad (25)$$

Using expression (11) for the retarded self-energy, the following equation of motion for the retarded Green's function $\mathbf{G}_{CC}^r(t_1, t_2)$ is obtained:

$$\left(i \frac{d}{dt_1} - \mathbf{h}_{CC}^{eff} \right) \mathbf{G}_{CC}^r(t_1, t_2) = \mathbf{1}_{CC} \delta(t_1 - t_2) \quad (26)$$

It immediately follows from this equation that the retarded Green's function depends only on the time difference. This is a direct consequence of the fact that the retarded self-energy is proportional to the delta function. Therefore, one can introduce in the usual way the Fourier transform of the retarded Green's function,

$$\mathbf{G}_{CC}^r(\omega) = \left(\omega \mathbf{1}_{CC} - \mathbf{h}_{CC}^{eff} \right)^{-1} \quad (27)$$

The matrix \mathbf{h}_{CC}^{eff} is not Hermitian; however, one can define its left and right eigenvectors which share the same eigenvalues. Using then the corresponding spectral representation of this matrix and integrating over ω in the complex plane, the time representation of the retarded Green's function is obtained:

$$\mathbf{G}_{CC}^r(t_1, t_2) = -i\theta(t_1 - t_2) e^{-i\mathbf{h}_{CC}^{eff}(t_1-t_2)} \quad (28)$$

A similar calculation for the advanced Green's function yields:

$$\mathbf{G}_{CC}^a(\omega) = \left(\omega \mathbf{1}_{CC} - \left(\mathbf{h}_{CC}^{eff} \right)^\dagger \right)^{-1} \quad (29)$$

$$\mathbf{G}_{CC}^a(t_1, t_2) = i\theta(t_2 - t_1) e^{-i(\mathbf{h}_{CC}^{eff})^\dagger(t_1-t_2)} \quad (30)$$

We see that even in the case of the variable bias the retarded and advanced functions do not depend on the bias in the WBLA and hence it is not surprising that they have exactly the same form as in [8].

2.4.4 The lesser Green's function

Projecting Eqs. (6) and (7) onto the lesser component, using the Langreth rules and the known expression for the retarded self-energy (11), the following equations of motion for the lesser Green's function are obtained:

$$\left(i \frac{d}{dt_1} - \mathbf{h}^{eff}\right) \mathbf{G}^<(t_1, t_2) = (\boldsymbol{\Sigma}^< \cdot \mathbf{G}^a + \boldsymbol{\Sigma}^\nabla \star \mathbf{G}^\nabla)_{(t_1, t_2)} \quad (31)$$

$$\mathbf{G}_{CC}^<(t_1, t_2) \left[-i \frac{d}{dt_2} - (\mathbf{h}_{CC}^{eff})^\dagger\right] = (\mathbf{G}_{CC}^r \cdot \boldsymbol{\Sigma}_{CC}^< + \mathbf{G}_{CC}^\nabla \star \boldsymbol{\Sigma}_{CC}^\nabla)_{(t_1, t_2)} \quad (32)$$

where for simplicity of notations we have omitted the CC subscript in all matrices above as they are defined on the orbitals of the central region only and hence there should be no ambiguity. We shall retain this simplified notations in what follows.

We now look to put the WBLA Kadanoff-Baym equations for the lesser Green's Functions into a form suitable for the integration. This is done by introducing the "tilded" function $\tilde{\mathbf{G}}^<(t_1, t_2)$ via the following transformation (similar to the canonical transformation performed in [8] for the equal time case):

$$\mathbf{G}_{CC}^<(t_1, t_2) = e^{-i\mathbf{h}_{CC}^{eff}(t_1-t_0)} \tilde{\mathbf{G}}_{CC}^<(t_1, t_2) e^{i(\mathbf{h}_{CC}^{eff})^\dagger(t_2-t_0)}$$

Differentiating both sides with respect to either t_1 or t_2 and using the above equations of motion, we can calculate the partial derivatives of the tilded function with respect to both times:

$$\frac{\partial \tilde{\mathbf{G}}_{CC}^<(t_1, t_2)}{\partial t_1} = -ie^{i\mathbf{h}_{CC}^{eff}(t_1-t_0)} (\boldsymbol{\Sigma}_{CC}^< \cdot \mathbf{G}_{CC}^a + \boldsymbol{\Sigma}_{CC}^\nabla \star \mathbf{G}_{CC}^\nabla)_{(t_1, t_2)} e^{-i(\mathbf{h}_{CC}^{eff})^\dagger(t_2-t_0)} \quad (33)$$

$$\frac{\partial \tilde{\mathbf{G}}_{CC}^<(t_1, t_2)}{\partial t_2} = ie^{i\mathbf{h}_{CC}^{eff}(t_1-t_0)} (\mathbf{G}_{CC}^r \cdot \boldsymbol{\Sigma}_{CC}^< + \mathbf{G}_{CC}^\nabla \star \boldsymbol{\Sigma}_{CC}^\nabla)_{(t_1, t_2)} e^{-i(\mathbf{h}_{CC}^{eff})^\dagger(t_2-t_0)} \quad (34)$$

We explicitly prove in Appendix A that the mixed second derivatives of the tilded function do not depend on the order of differentiation. Therefore, one can introduce the exact differential

$$d\tilde{\mathbf{G}}^<(t_1, t_2) = \mathbf{F}^{(1)}(t_1, t_2) dt_1 + \mathbf{F}^{(2)}(t_1, t_2) dt_2$$

so that $\tilde{\mathbf{G}}^<(t_1, t_2)$ can be calculated using a line integral taken along an arbitrary path connecting the initial, (t_0, t_0) , and the final, (t_1, t_2) , points in the two-dimensional (t_1, t_2) plane. In Appendix B, details are given on how to perform the line integral which results in the following final expression for the lesser Green's function of two times:

$$\begin{aligned} \mathbf{G}^<(t_1, t_2) = e^{-i\mathbf{h}^{eff}(t_1-t_0)} \int \frac{d\omega}{2\pi} f(\omega - \mu) \sum_{\alpha} [\mathbf{K}_{\alpha}(t_1, t_0; \omega) \boldsymbol{\Gamma}_{\alpha} \mathbf{G}^a(\omega) - \mathbf{G}^r(\omega) \boldsymbol{\Gamma}_{\alpha} \mathbf{K}_{\alpha}^{\dagger}(t_2, t_0; \omega) \\ + i\mathbf{K}_{\alpha}(t_1, t_0; \omega) \boldsymbol{\Gamma}_{\alpha} \mathbf{K}_{\alpha}^{\dagger}(t_2, t_0; \omega) + i\mathbf{A}_{\alpha}(\omega)] e^{i(\mathbf{h}^{eff})^\dagger(t_2-t_0)} \end{aligned} \quad (35)$$

Above, we have introduced the spectral function $\mathbf{A}_{\alpha}(\omega) = \mathbf{G}^r(\omega) \boldsymbol{\Gamma}_{\alpha} \mathbf{G}^a(\omega)$ for the α lead, and defined the following matrix object:

$$\mathbf{K}_{\alpha}(t, t_0; \omega) = \int_{t_0}^t d\bar{t} e^{-i(\omega \mathbf{1} - \mathbf{h}^{eff})(\bar{t}-t_0)} e^{-i\psi_{\alpha}(\bar{t}, t_0)} \quad (36)$$

which contains all the effects related to the variable bias.

The general result obtained for the lesser Green's function allows calculation of the current through any lead which will be done in the next section. Here we shall mention that another observable of great interest which can be directly calculated from the Green's function is the central region density matrix $\rho(t) = -i\mathbf{G}^<(t, t)$.

Note that in [8] only the equal time lesser Green's function was derived as this is sufficient to calculate the current in WBLA. However, the two-time Green's function may be required for the calculation of other physical quantities, e.g. for the calculation of the noise [40]), and hence we have provided the general result here.

2.5 The current

2.5.1 Generalized LB formula

The LB formula for the current in lead α is obtained within the NEGF formalism as the long-time limit of the quantity $2q \left\langle \frac{d\hat{N}_{\alpha}(t)}{dt} \right\rangle$ following a static bias switch-on[30, 8], where $\hat{N}_{\alpha}(t) = \sum_k \hat{d}_{k\alpha}^{\dagger} \hat{d}_{k\alpha}$ is the number operator of this lead. Using

the equation of motion for the number operator, it can be shown that, for all times, this current is given by the following expression [8]:

$$I_\alpha(t) = 4qReTr_C [\mathbf{h}_{C\alpha} \mathbf{G}_{\alpha C}^<(t, t)]$$

One then applies the Langreth theorem to the Dyson equation for $\mathbf{G}_{\alpha C}^<(t, t)$ to obtain:

$$I_\alpha(t) = -4ReTr_C \left[(\Sigma_\alpha^< \cdot \mathbf{G}^a + \Sigma_\alpha^r \cdot \mathbf{G}^< + \Sigma_\alpha^\top \star \mathbf{G}^\Gamma)_{(t,t)} \right] \quad (37)$$

where the trace is taken with respect to the orbitals of the central region and we set the charge of an electron to -1 . This expression in its right hand side contains the sum of three convolution integrals defined by Eqs. (22) and (19). Let us consider briefly the physical meaning of each term in this current formula. $\Sigma_\alpha^<$ is proportional to the decoupled lesser Green's function of the α lead, and therefore to the probability of finding an electron in the leads, whereas \mathbf{G}^a is a two-time propagator. So $\Sigma_\alpha^< \cdot \mathbf{G}^a$ is interpreted as a 'source' term: it gives the current due to electrons tunneling from lead α into the central region[34]. The $\Sigma_\alpha^r \cdot \mathbf{G}^<$ term, by contrast, is a 'sink' term: it contains $\mathbf{G}^<$, which is proportional to the probability of occupation of the C region, and may therefore be attributed to the tunneling of electrons out from the central region[29, 34]. Finally, $\Sigma_\alpha^\top \star \mathbf{G}^\Gamma$ is a term containing information on the coupled system prior to the switch on time t_0 . As such, it vanishes in the partitioned approach, and the formula (37) reduces to the expression used in Ref. [29]. Within the WBLA, all functions of two times appearing in these convolution integrals are known, so that after some lengthy but simple algebra the current evaluates to the following:

$$\begin{aligned} I_\alpha(t) = 2i \int \frac{d\omega}{2\pi} f(\omega - \mu) Tr_C \left\{ \Gamma_\alpha e^{i(\omega 1 - \mathbf{h}^{eff})(t-t_0)} e^{i\psi_\alpha(t, t_0)} [\mathbf{G}^r(\omega) - i\mathbf{K}_\alpha(t, t_0; \omega)] \right. \\ \left. - \Gamma_\alpha [\mathbf{G}^a(\omega) + i\mathbf{K}_\alpha^\dagger(t, t_0; \omega)] e^{-i(\omega 1 - \mathbf{h}^{eff})^\dagger(t-t_0)} e^{-i\psi_\alpha(t, t_0)} + \Gamma_\alpha e^{-i\mathbf{h}^{eff}(t-t_0)} \sum_{\alpha'} \left[i\mathbf{K}_{\alpha'}(t, t_0; \omega) \Gamma_{\alpha'} \mathbf{K}_{\alpha'}^\dagger(t, t_0; \omega) \right. \right. \\ \left. \left. + \mathbf{K}_{\alpha'}(t, t_0; \omega) \Gamma_{\alpha'} \mathbf{G}^a(\omega) - \mathbf{G}^r(\omega) \Gamma_{\alpha'} \mathbf{K}_{\alpha'}^\dagger(t, t_0; \omega) + i\mathbf{A}_{\alpha'}(\omega) \right] e^{i(\mathbf{h}^{eff})^\dagger(t-t_0)} \right\} \quad (38) \end{aligned}$$

This expression enables us to model electron transport in response to the switch-on of an arbitrary time-dependent bias, within the WBLA.

2.5.2 Recovery of known results: asymptotics

Without making any assumptions on the shape of the bias, it is instructive to investigate the long time behaviour of the expression (38), which can be done by taking the limit $t_0 \rightarrow -\infty$, i.e. we shift the switch-on time to the distant past. We first note that, as $t_0 \rightarrow -\infty$, the asymptotic value of the 'preparation' term,

$$\Sigma_\alpha^\top \star \mathbf{G}^\Gamma(t, t) = i \int \frac{d\omega}{2\pi} f(\omega - \mu) \Gamma_\alpha \mathbf{G}^a(\omega) e^{-i(\omega 1 - \mathbf{h}_{CC}^{eff})^\dagger(t-t_0)}$$

which contains the matrix function $e^{-i(\omega 1 - \mathbf{h}_{CC}^{eff})^\dagger(t-t_0)} \propto e^{\Gamma t_0/2}$, is vanishing ($\Gamma > 0$), so that it has no effect on the steady state current. To investigate other objects associated with the system preparation, we consider those terms which result from vertical contour convolutions in $\mathbf{G}^<$ (i.e. terms arising from $\mathcal{G}^{(2)}$ and $\mathcal{G}^{(4)}$ in Appendix B):

$$\lim_{t_0 \rightarrow -\infty} \left[e^{-i\mathbf{h}_{CC}^{eff}(t-t_0)} (\mathbf{K}_\alpha(t, t_0; \omega) \Gamma_\alpha \mathbf{G}^a(\omega) - \mathbf{G}^r(\omega) \Gamma_\alpha \mathbf{K}_\alpha^\dagger(t, t_0; \omega)) e^{i(\mathbf{h}_{CC}^{eff})^\dagger(t-t_0)} \right] = 0$$

also due to the $e^{\Gamma t_0/2}$ term; note that all times in the integral domain of \mathbf{K}_α are less than or equal to t . In addition, the term which arises from the initial condition for the integral of the lesser Green's function,

$$\lim_{t_0 \rightarrow -\infty} \left[e^{-i\mathbf{h}_{CC}^{eff}(t-t_0)} \mathbf{A}_\alpha(\omega) e^{i(\mathbf{h}_{CC}^{eff})^\dagger(t-t_0)} \right] = 0$$

also vanishes in this limit as it also contains a similar exponential factor of $e^{\Gamma t_0}$. The asymptotic behaviour of the current for an arbitrary time-dependent bias is therefore given by:

$$\begin{aligned} \lim_{t_0 \rightarrow -\infty} I_\alpha(t) = \lim_{t_0 \rightarrow -\infty} 2 \int \frac{d\omega}{2\pi} f(\omega - \mu) Tr_C \left\{ \Gamma_\alpha \left(e^{i(\omega 1 - \mathbf{h}^{eff})(t-t_0)} e^{i\psi_\alpha(t, t_0)} \mathbf{K}_\alpha(t, t_0; \omega) \right. \right. \\ \left. \left. + \mathbf{K}_\alpha^\dagger(t, t_0; \omega) e^{-i(\omega 1 - \mathbf{h}^{eff})^\dagger(t-t_0)} e^{-i\psi_\alpha(t, t_0)} - e^{-i\mathbf{h}^{eff}(t-t_0)} \sum_{\alpha'} \mathbf{K}_{\alpha'}(t, t_0; \omega) \Gamma_{\alpha'} \mathbf{K}_{\alpha'}^\dagger(t, t_0; \omega) e^{i(\mathbf{h}^{eff})^\dagger(t-t_0)} \right) \right\} \quad (39) \end{aligned}$$

where the limit remains on the right-hand side to account for the possibility of decaying terms once the bias has been specified, and we remark that in this limit the current remains a variable function of t .

In the formula (39), all terms resulting from either the equilibrium initial condition or from vertical contour convolutions have vanished. This tells us that the long-time limit of the current is independent of the way the system was prepared, and highlights the advantages of using a contour formalism, in which all preparation-dependent terms can be easily identified. Furthermore, with the exception of the initial condition term, every vanishing term includes a convolution with a left or right self-energy. In the partitioned approach to the transport problem, these quantities vanish, as one can see from the definition (8) and $\mathbf{h}_{C\alpha}(t_0 - i\tau) = 0$. So the formula (39) tells us that, at long times, the partitioned approach yields the same current as in the partition-free treatment. If one is interested in the transient regime, however, only the latter approach will yield a physical current.

At this point, we can make a precise connection with the results of Jauho et. al., who considered the switch-on of a time-dependent bias taking place at $t_0 = -\infty$ within a partitioned approach[29]. They solved the Dyson equations on a two-branch contour running from $-\infty$ to t , before returning to $-\infty$ on a lower time branch, and obtained the following expression for the lesser Green's function of two times:

$$\mathbf{G}^<(t_1, t_2) = \int_{-\infty}^t \int d\bar{t} d\bar{t}' \mathbf{G}^r(t_1, \bar{t}) \boldsymbol{\Sigma}^<(\bar{t}, \bar{t}') \mathbf{G}^a(\bar{t}', t_2)$$

where the functional form of the retarded/advanced Green's functions is identical to (28), (30). Working within the WBLA, and neglecting any time-dependence of the coupling, we can re-write this in the form:

$$\mathbf{G}^<(t_1, t_2) = \lim_{t_0 \rightarrow -\infty} e^{-i\mathbf{h}_{CC}^{eff}(t_1-t_0)} \int \frac{d\omega}{2\pi} f(\omega - \mu) \sum_{\alpha} i\mathbf{K}_{\alpha}(t_1, t_0; \omega) \boldsymbol{\Gamma}_{\alpha} \mathbf{K}_{\alpha}^{\dagger}(t_2, t_0; \omega) e^{i(\mathbf{h}_{CC}^{eff})^{\dagger}(t_2-t_0)} \quad (40)$$

Working on the Keldysh contour used by Jauho et. al., one neglects imaginary time convolutions when applying the Langreth Rules, to get instead of (38) the following expression for the current:

$$I_{\alpha}(t) = -4Re \text{Tr}_C \left[(\boldsymbol{\Sigma}_{\alpha}^< \cdot \mathbf{G}^a + \boldsymbol{\Sigma}_{\alpha}^r \cdot \mathbf{G}^<)_{(t,t)} \right] \quad (41)$$

where the real-time convolutions now extend from $-\infty$ up to t . Inserting (40) into (41) and working within the WBLA, one can easily show that the resulting formula is given exactly by (39). This discussion clearly shows that the formula derived in [29] is approximate as it is missing the terms related to the initial preparation of the system.

2.5.3 Recovery of known results: static bias

A second important check on the general formula (38) is that it reduces to known expressions for the time-dependent current in the case of a time-independent bias after the switch-on. When the bias V_{α} is static after the switch on, (38) can be evaluated purely in terms of the retarded/advanced Green's functions of the central region, as in this case,

$$\mathbf{K}_{\alpha}(t_1, t_0; \omega) = i\mathbf{G}^r(\omega + V_{\alpha}) \left[e^{-i((\omega+V_{\alpha})\mathbf{1}-\mathbf{h}_{CC}^{eff})(t_1-t_0)} - \mathbf{1} \right] \quad (42)$$

$$\mathbf{K}_{\alpha}^{\dagger}(t_2, t_0; \omega) = -i \left[e^{i((\omega+V_{\alpha})\mathbf{1}-\mathbf{h}_{CC}^{eff})^{\dagger}(t_2,t_0)} - \mathbf{1} \right] \mathbf{G}^a(\omega + V_{\alpha}) \quad (43)$$

Substituting these expressions into Eq. (35), it is found to reduce to the following formula:

$$\begin{aligned} \mathbf{G}^<(t_1, t_2) &= i \sum_{\alpha} \frac{d\omega}{2\pi} f(\omega - \mu) \left[\mathbf{A}_{\alpha}(\omega + V_{\alpha}) e^{-i(\omega+V_{\alpha})(t_1-t_2)} \right. \\ &+ V_{\alpha} \left(e^{-i\mathbf{h}^{eff}(t_1-t_0)} \mathbf{G}^r(\omega) \mathbf{A}_{\alpha}(\omega + V_{\alpha}) e^{i(\omega+V_{\alpha})(t_2-t_0)} + e^{-i(\omega+V_{\alpha})(t_1-t_0)} \mathbf{A}_{\alpha}(\omega + V_{\alpha}) \mathbf{G}^a(\omega) e^{i(\mathbf{h}^{eff})^{\dagger}(t_2-t_0)} \right) \\ &\left. + V_{\alpha}^2 e^{-i\mathbf{h}^{eff}(t_1-t_0)} \mathbf{G}^r(\omega) \mathbf{A}_{\alpha}(\omega + V_{\alpha}) \mathbf{G}^a(\omega) e^{i(\mathbf{h}^{eff})^{\dagger}(t_2-t_0)} \right] \quad (44) \end{aligned}$$

We remark that this expression is not, in general, a function of the time difference $\tau \equiv t_1 - t_2$. This property is satisfied only when both (a) $t_0 \rightarrow -\infty$ (or $t_1, t_2 \rightarrow \infty$) and (b) \mathbf{h}_{CC} commutes with $\boldsymbol{\Gamma}$, in which case the Fourier transform of (44) is a function of a single frequency. If one sets $t_1 = t_2$, (44) reduces to the expression published in Refs. [8, 34, 33] for the equal-time case. This can be used to extract the particle number density of the central region via $\rho(t) = -i\mathbf{G}^<(t, t)$.

The LB formalism was initially developed for the treatment of junctions having a static bias placed across them. If one replaces $\mathbf{K}_{\alpha}, \mathbf{K}_{\alpha}^{\dagger}$ with those given in Eqs. (42) and (43), one recovers the expression reported in [[34]]. If one then inserts

these expressions into (39) and takes the right-hand limit, one obtains a Landauer-type formula for the multi-terminal junction [8]:

$$I_\alpha^{(LB)} = \lim_{t_0 \rightarrow -\infty} I_\alpha(t) = 2 \sum_{\alpha'} \int \frac{d\omega}{2\pi} [f(\omega - \mu - V_\alpha) - f(\omega - \mu - V_{\alpha'})] \text{Tr}_C \left[\mathbf{T}^{(\alpha\alpha')}(\omega) \mathbf{T}^{\dagger(\alpha\alpha')}(\omega) \right] \quad (45)$$

Here we have defined the transmission matrix:

$$\mathbf{T}^{(\alpha\alpha')}(\omega) \equiv [\mathbf{\Gamma}_\alpha]^{1/2} \mathbf{G}^r(\omega) [\mathbf{\Gamma}_{\alpha'}]^{1/2}$$

$\mathbf{T}^{(\alpha\alpha')}(\omega)$ is naturally interpreted as the probability amplitude for an electron to hop from lead α' to lead α , so that the current in lead α is just the sum over all frequencies of the rate at which electrons in lead α hop into α' , minus the rate at which electrons in lead α' hop into α . As all dependence on t has vanished in the long-time and static bias limits, these rates are also fixed for all times.

3 Results

To illustrate the general formula (38) derived above, we specialize the discussion to that of resonant tunneling through a single-level quantum dot, coupled to just two leads, L and R. The Hamiltonian matrix \mathbf{h}_{CC} of the central region is given by the scalar $h = \varepsilon_0$, and all other matrices defined on the central region also become scalars. In addition, we assume that the two leads are symmetric, i.e. the coupling is the same: $\Gamma_L = \Gamma_R = \frac{1}{2}\Gamma$. We choose our zero of energy to be equal to the chemical potential by setting $\mu = 0$. Thus the intrinsic frequency scales of the system are given by the difference $|\varepsilon_0 - \mu|$ and by Γ . The temperature is set to a value which is an order of magnitude smaller than any other characteristic energy of the problem: $k_B T = 0.1$.

We consider a bias in the left lead that is switched on instantaneously and thereafter sinusoidally varying in time with frequency Ω_L about a fixed value V_L , and a bias in the right lead that is set to zero:

$$V_L(t) = V_L + A_L \cos(\Omega_L t), \quad V_R(t) = 0, \quad t \geq t_0 = 0 \quad (46)$$

Either bias is zero at $t < 0$. This particular choice of the bias introduces two new energy scales into the problem: firstly, there is an intrinsic energy difference of $|\mu + V_L - \varepsilon_0|$ between the fixed point of the left lead Fermi level and the dot energy. In addition, there is a new energy scale set by the driving frequency Ω_L . When $A_L \neq 0$, this driving frequency causes the Fermi level of L to vary on a timescale that is slower than the inverse plasmon frequency ω_p of the leads, so that at each time step there is a new energy gap which must be traversed for electron hopping between the quantum dot and the lead L to occur.

To evaluate the current in the left lead we use a well-known expression for the generating function for the n -th order Bessel functions of the first kind $J_n(z)$, so that the time integrals can be calculated analytically (cf. [29]). This puts the K_L time integral (36) into the form

$$K_L(t, 0; \omega) = i \sum_{n=-\infty}^{\infty} J_n\left(\frac{A_L}{\Omega_L}\right) G^r(\omega + V_L + n\Omega_L) \left[e^{-i(\omega + V_L + n\Omega_L - h^{eff})t} - 1 \right] \quad (47)$$

where $h^{eff} = h - i\Gamma/2$, while the K_R integral is simply

$$K_R(t, 0; \omega) = i G^r(\omega) \left[e^{-i(\omega - h^{eff})t} - 1 \right] \quad (48)$$

These are substituted into (38) to yield a frequency integral for the time-dependent current, which may then be calculated numerically, and we shall plot in the following the resulting current in the left lead, $I_L(t)$, for various combinations of the parameters of the problem. These plots will also exhibit the suitably normalized time dependent bias (dotted line) as well as the prediction of the current calculated using the steady-state (SS) expression for the current at the instantaneous value of the bias (red line):

$$I_L^{(LB)} = \frac{\Gamma^2}{2} \int \frac{d\omega}{2\pi} \frac{[f(\omega - V - \mu) - f(\omega - \mu)]}{(\omega - \varepsilon_0)^2 + (\Gamma/2)^2} \quad (49)$$

The exact time-dependent (TD) current response calculated using our new formula will be shown by a black line. Comparison of the exact current with the one calculated using the SS expression is intended to illustrate the additional effects that can be captured with an exact TD approach.

We illustrate the set-up schematically in Fig. 3(a) for the parametrisation $\varepsilon_0 = 1$, $\mu = 0$, $V_L = 5$ and $A_L = 4$. In this particular case, the effect of the bias is to cause the Fermi level of the left lead to move down and 'touch' the dot energy, before being removed far away from ε_0 . The corresponding time-dependence of the current is displayed in Fig. 3(b) for $\Gamma = 1$ and $\Omega_L = 1$. It has several features in common with all calculated currents we shall discuss below.

To understand the SS current, we need only take the zero temperature limit of the formula (45) for the two lead case we are considering. This gives the following expression for the current:

$$\lim_{t_0 \rightarrow -\infty, T \rightarrow 0} I_L(t) = \frac{\Gamma}{2\pi} \left[\arctan \left[\frac{\mu + V_L - \varepsilon_0}{\Gamma/2} \right] - \arctan \left[\frac{\mu - \varepsilon_0}{\Gamma/2} \right] \right] \quad (50)$$

This has a roughly linear or ohmic behaviour when the chemical potential is within $\frac{1}{2}\Gamma$ of ε_0 and saturates otherwise, as seen in the red curve in Fig. 3(b). The curve follows the bias for low bias, but is cut-off at higher bias.

Our results on the TB current show a rapidly varying transient that relaxes to a periodic steady-state solution on a timescale of $2/\Gamma$, a fact which can be predicted from the terms multiplied by exponential factors $e^{-\Gamma t}$ and $e^{-\Gamma t/2}$ in the analytic formula for the current we derived (see Appendix C for the details of this formula). All plots therefore exhibit at least two effects: the transient reaction to the switch-on event and the time-varying current due to the persistent bias oscillations. This much can be seen from the graph in Fig. 3(b), where for times greater than $2/\Gamma$, the current response is periodic with a period of $\tau_L = 2\pi/\Omega_L$. In addition to these two features, we observe a 'ringing' oscillation of the current (first observed in Ref. [29]) occurring within each period, leading to asymmetry of the current about those voltage peaks located at multiples of 2π . This 'ringing' signal is evidence of an internal frequency of the system at which resonances in the current signal occur on a shorter timescale than τ_L . It consists of a series of peaks which are damped consecutively before tending to flatten, and which then agree for a short time with the steady-state formula. We also observe that, although the steady-state current is always in phase with the voltage, the minimum of the exact current is delayed with respect to the voltage.

Let us first consider the effect on this system of varying the dot energy level. This is done in steps of unit energy, and the resulting plots for the current as a function of time are shown in Fig. 4(a)-(d). It is clear from these plots that the frequency of the 'ringing' oscillations of the TD current is determined by the position of the dot relative to the two Fermi levels. In particular, it seems that the frequency of these oscillations is roughly equal to the energy gap $|\mu + V_L - \varepsilon_0|$, as each unit increase in ε_0 tends to flatten or remove a peak from the 'ringing' transient. The dependence of this effect on the left gap alone can be checked by moving V_L and ε_0 by the same amount; indeed our calculations demonstrate that this leaves the number of 'ringing' peaks unchanged. When the gap $|\mu + V_L - \varepsilon_0|$ is equal to zero, Fig. 4(d), the 'ringing' ceases to be significant, although an asymmetric peak after the minimum of the bias is still present, as discussed above. This is not surprising, because when $\varepsilon_0 = V_L$ the time-dependent shift in the Fermi level of the left lead is symmetric about ε_0 . Physically, we interpret the 'ringing' current signal as an outcome of competing intrinsic timescales: the timescale of tunnelling from the left lead onto the dot is smaller than the typical lifetime of an electron in the dot state, given by $\tau_{el} \sim 2/\Gamma$. It is apparent from the Figs. 4(a)-(d) that the possibility for a negative current is also determined by the position of the dot energy relative to the left Fermi level, and that the minima of the current become increasingly negative as ε_0 is brought closer to V_L .

Next, we consider the effects on the current response of varying the driving frequency. One would intuitively expect that, as the driving frequency of the bias is lowered, the agreement between our TD formula and the LB formula for the SS current becomes better as the bias varies more slowly, suggesting that the LB formula derived for the case of a static bias would become appropriate. In Fig. 5, all parameters, except for the bias frequency, are the same as in Fig. 3(b). In (a) the driving frequency of the bias was scaled down to $\Omega_L = 0.1$. One can see that in this adiabatic limit there is excellent agreement with the steady-state formula, with the exception of a quickly oscillating transient following t_0 , and a very quickly suppressed single 'ringing' peak. In Fig. 5(b), the driving frequency is scaled up to $\Omega_L = 10$, with the effect that the current response deviates significantly from that given by the LB formula. Interestingly, in this high frequency case it takes around 4 to 5 bias cycles for the current to stabilise into steady oscillations. In addition, a phase-shift of the current response with respect to the steady-state value is clearly visible. During the transient regime, the amplitude of the exact current disagrees with the steady state current at all times. The amplitude of the exact current at the bias peaks is much greater than the amplitude of the steady state current in the long-time regime.

In Fig. 6 we consider the effect of varying the level width Γ , where all other parameters are fixed at the same values as in Fig. 3(b). As discussed above, this quantity fixes the timescale over which the transient current decays. We display the effects of setting $\Gamma = 0.2$ in panel (a). We see that this has the effect of prolonging the transient and of accentuating the 'ringing' peaks in the TD current, without adding any new peaks to this part of the signal. In Fig. 6(b) the level width $\Gamma = 5.0$; we see that for $t > 2.5 = \tau_{el}$, the TD formula is periodic, but it is also interesting to note that the 'ringing' oscillations are greatly suppressed, in a manner which is qualitatively similar to the suppression observed above for an adiabatic driving frequency, Fig. 5(a). Interpreting Γ as the frequency with which electrons tunnel off the dot, we see that in this case it is greater than any other typical energy gap in the problem, so that the time scale with which electrons tunnel onto the dot is greater than that with which they escape.

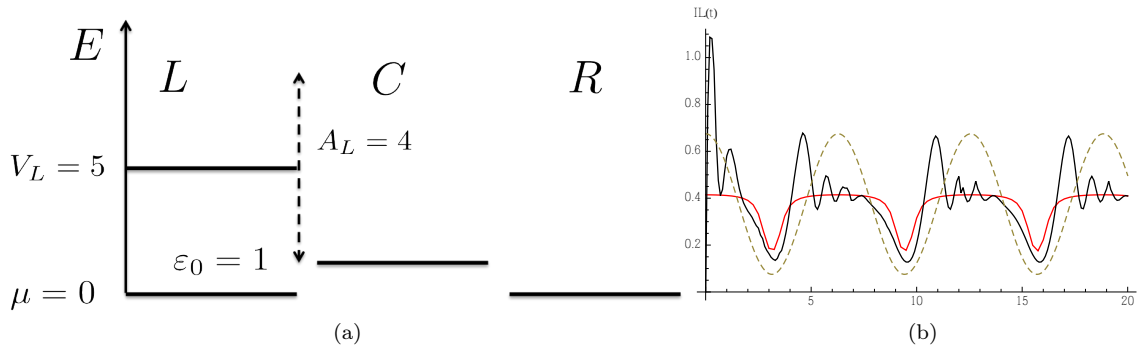


Figure 3: The basic system we are considering, with parameters $\Gamma = 1$, $\varepsilon_0 = 1$, $\mu = 0$, $V_L = 5$, $A_L = 4$, $\Omega_L = 1$. This system is illustrated schematically in (a), and the time-dependent current through this system shown in (b).

We also investigate the effect of decreasing the amplitude A_L of the bias oscillations about the fixed point V_L , and the result for $A_L = 2$ is shown in Fig. 7. The main effects observed in Fig. 3(b) are present, but as the left Fermi level never comes all the way down to ‘touch’ ε_0 , there is relatively little ‘ringing’ in the TD current in addition to the SS behaviour. In the temperature regime we are considering, Eq. (50) is in close agreement with the SS formula at all values of the time-dependent bias inserted into V_L . Large variations of the bias bring it closer to ε_0 , where the arctan function varies most rapidly. For an oscillation amplitude that simply moves the bias by a small amount around a value of V_L which is much larger than ε_0 , the SS current will move up and down an asymptote of the arctan function and remain almost static, becoming completely static as $A_L \rightarrow 0$.

Finally, we can see in Fig. 8 that increasing the system temperature so that $k_B T = 1.0$ has the effect of suppressing the ‘ringing’ peaks on the current signal. Increasing the temperature thus has a qualitatively similar effect to an increase in Γ .

4 Conclusions

In this paper, we have considered, within a tight binding model, electron conduction in a multi-terminal system following the switch-on of a time dependent bias. Our formalism, which mostly relies on the method developed in Refs. [32, 37, 34, 8, 33], is an example of a partition-free approach, whereby the whole system is fully coupled prior to the bias switch on.

We showed that within the WBLA it is possible to solve the corresponding Kadanoff-Baym equations for all components of the Non-Equilibrium Green’s Functions and derive a closed expression for the current in such a system. Our formula for the current includes both transient effects due to the switch-on and the current time variation due to the time-dependent bias in each lead, subsequent to the switch-on. We showed that our formula reduces to a number of known results previously obtained: (i) by taking the switch on time t_0 to $-\infty$, our formula coincides with the result of Jauho *et al.* [29] where a partitioned approach was used; (ii) assuming the bias is static after the switch on, we recover the result of Stefanucci *et al* [32, 8].

Moreover, it was also possible to state the conditions under which the partitioned and partition-free approaches would yield identical results within the WBLA, and to show that the long-time limit of the time-dependent current satisfies these conditions. Therefore, as expected [32, 8], in the long time limit the expression for the current due to a constant bias approaches the well-known Landauer steady-state result.

The analytical result for the current we have obtained enabled us to isolate terms in the current which are associated with the system preparation, and to study the long-time behaviour of the current. Note that in this case the bias is still time dependent, but all effects of the switch on have been eliminated.

Finally we have applied the formalism developed to the case of an AC bias placed across a single-level resonant tunneling device, with results that reduce to the steady-state LB formalism in the case where the driving field is varied adiabatically slowly. We have also looked at effects of the position of the dot energy level with respect to the Fermi levels of the unbiased leads and showed that the number of ‘ringing’ oscillations in the current appearing at the beginning of each bias peak is directly related to the position of the dot level. Dependence of the current on the oscillation amplitude of the bias, the temperature, and the coupling between the leads and the central system (the ‘level width’) has also been analysed.

We anticipate that this formalism will be applicable to the study of TD conductance and current fluctuations through magnetic systems describable by one-particle Hamiltonians (including those extracted from self-consistent density-functional approaches).

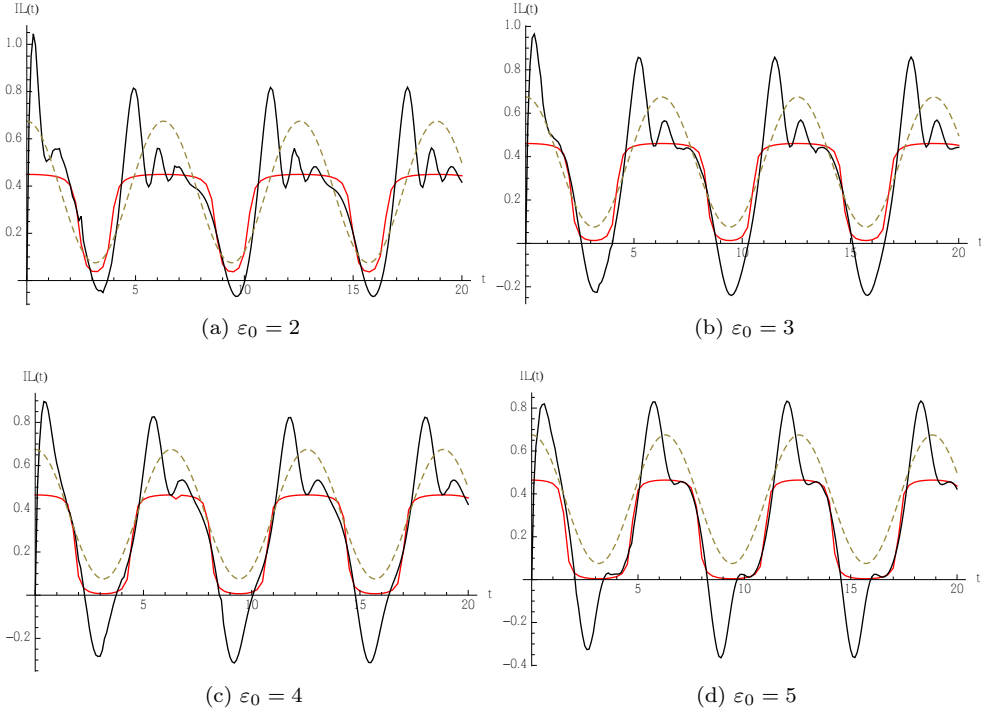


Figure 4: The effect of varying the dot energy. As ε_0 is moved closer to V_L , the intrinsic frequency of the 'ringing' oscillations is increased. When these two energies are aligned, the current response is symmetric about $I_L \sim 0.225$, because the movement of the left Fermi level is symmetric around ε_0 .

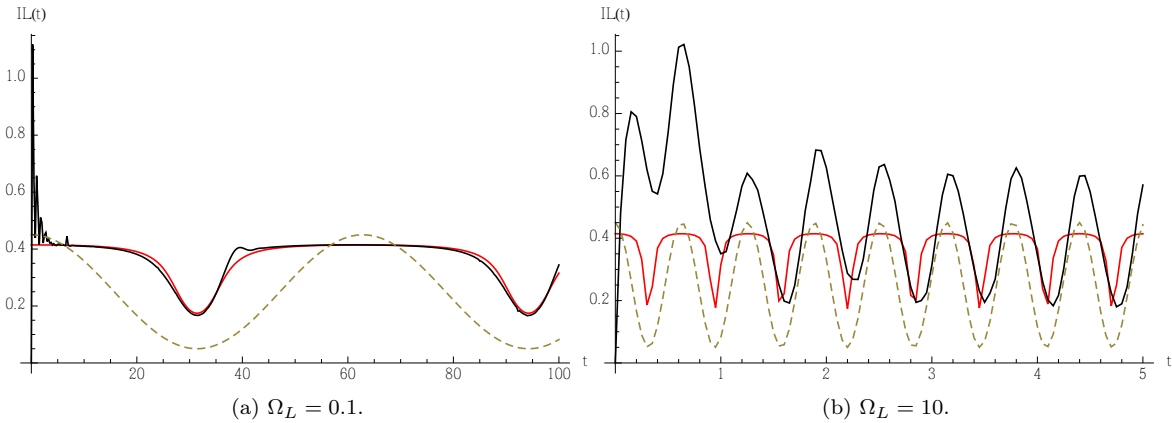


Figure 5: The effect of varying the driving frequency, with all other parameters as in Fig. 3(b). In (a), we see that our formula gives a good agreement with the steady-state LB formula, as this is tending towards the adiabatic limit. In (b), the high driving frequency causes the current to be phase-delayed, and also to strongly disagree with the LB formula in amplitude.

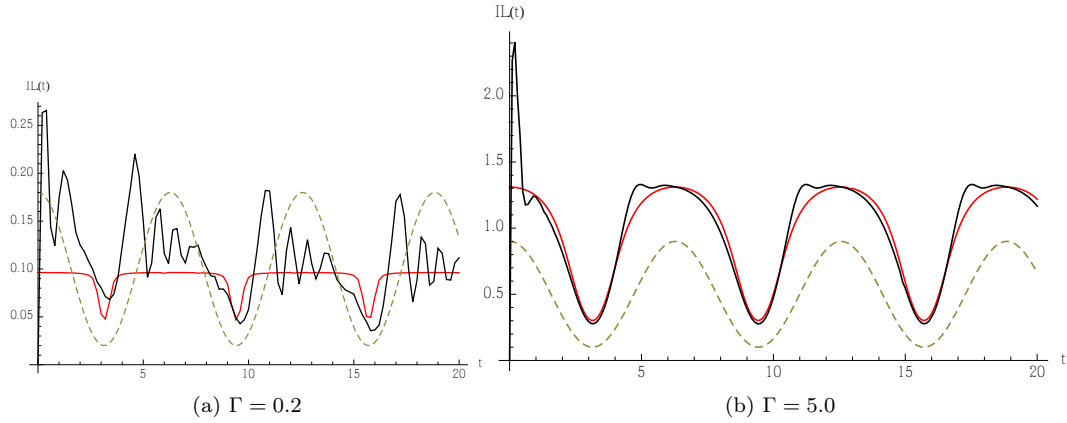


Figure 6: We exhibit the effects of varying the level width, where all other parameters as in Fig. 3(b). We find that Γ tends to suppress any non-adiabatic features as it increases in magnitude.

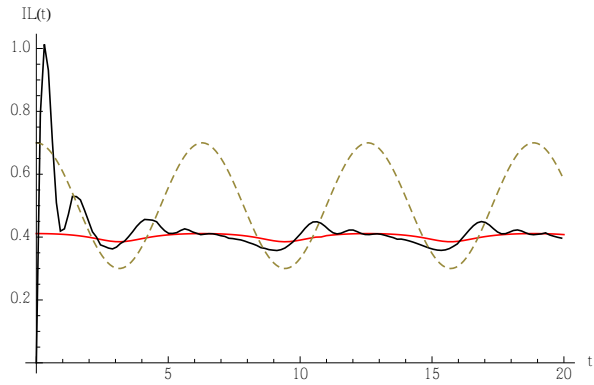


Figure 7: Effect on the current response of reducing the bias amplitude from $A_L = 4$ (as in Fig. 3(b)) to $A_L = 2$.

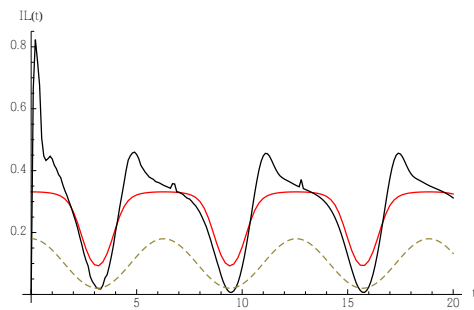


Figure 8: The high temperature behaviour of the current is investigated. Here we plot the TD current for $k_B T = 1.0$, and all other parameters are as in Fig. 3(b).

Acknowledgements Michael Ridley was supported through a studentship in the Centre for Doctoral Training on Theory and Simulation of Materials at Imperial College funded by the Engineering and Physical Sciences Research Council under grant number EP/G036888/1.

Appendix A - Path-independence

It is well-known from mathematics that a necessary and sufficient condition for the path-independence of a line integral $\int_L g(x, y)dx + h(x, y)dy$ on the (x, y) plane is $\partial g/\partial y = \partial h/\partial x$. This is equivalent to the statement that $df = gdx + hdy$ is an exact differential of some function $f(x, y)$. This condition corresponds to the symmetry of the second order mixed derivatives $\frac{\partial^2 f}{\partial x \partial y} = \frac{\partial^2 f}{\partial y \partial x}$ of this $f(x, y)$.

Green's functions are defined as functions of two contour times, i.e. the domain for integration of the Green's function is the set of points $\{(z_1, z_2) : z_1 \in \gamma \wedge z_2 \in \gamma\}$. We shall verify here that the mixed second derivatives of the Green's function $\mathbf{G}(z_1, z_2)$ are symmetric. We can write using the corresponding equations of motion (all matrices are given on the subspace of the central region and the subscript CC is omitted):

$$\begin{aligned}\frac{\partial \mathbf{G}(z_1, z_2)}{\partial z_1} &= -i \left[\mathbf{h}(z_1) \mathbf{G}(z_1, z_2) + \mathbf{1} \delta(z_1, z_2) + \int_{\gamma} d\bar{z} \mathbf{\Sigma}(z_1, \bar{z}) \mathbf{G}(\bar{z}, z_2) \right] \\ \frac{\partial \mathbf{G}(z_1, z_2)}{\partial z_2} &= i \left[\mathbf{G}(z_1, z_2) \mathbf{h}(z_2) + \mathbf{1} \delta(z_1, z_2) + \int_{\gamma} d\bar{z} \mathbf{G}(z_1, \bar{z}) \mathbf{\Sigma}(\bar{z}, z_2) \right]\end{aligned}$$

From the first of these:

$$\frac{\partial^2 \mathbf{G}(z_1, z_2)}{\partial z_2 \partial z_1} = -i \left[\mathbf{h}(z_1) \frac{\partial \mathbf{G}(z_1, z_2)}{\partial z_2} + \mathbf{1} \frac{\partial \delta(z_1, z_2)}{\partial z_2} + \int_{\gamma} d\bar{z} \mathbf{\Sigma}(z_1, \bar{z}) \frac{\partial \mathbf{G}(\bar{z}, z_2)}{\partial z_2} \right]$$

while from the second:

$$\frac{\partial^2 \mathbf{G}(z_1, z_2)}{\partial z_1 \partial z_2} = i \left[\frac{\partial \mathbf{G}(z_1, z_2)}{\partial z_1} \mathbf{h}(z_2) + \mathbf{1} \frac{\partial \delta(z_1, z_2)}{\partial z_1} + \int_{\gamma} d\bar{z} \frac{\partial \mathbf{G}(z_1, \bar{z})}{\partial z_1} \mathbf{\Sigma}(\bar{z}, z_2) \right]$$

Note that due to the order in which the Green's functions and self-energy appear to the right hand side of the derivatives, one never needs to consider derivatives of the self-energy. Noting next that $\frac{\partial \delta(z_1, z_2)}{\partial z_2} = -\frac{\partial \delta(z_1, z_2)}{\partial z_1}$, and making use of the first derivatives written above, we obtain that $\frac{\partial^2 \mathbf{G}(z_1, z_2)}{\partial z_2 \partial z_1} = \frac{\partial^2 \mathbf{G}(z_1, z_2)}{\partial z_1 \partial z_2}$.

Given this identity, we can take the lesser part of the Green's function by setting $z_1 = t_1 \in C_-$ and $z_2 = t_2 \in C_+$, which results in the required symmetry of the second order mixed derivatives for the CC -component of the lesser Green's function. This fact can be used to demonstrate that the same property is satisfied by the object

$$\tilde{\mathbf{G}}^<(t_1, t_2) \equiv e^{\mathbf{B}(t_1 - t_0)} \mathbf{G}^<(t_1, t_2) e^{\mathbf{B}^\dagger(t_2 - t_0)}$$

where \mathbf{B} is a square matrix, and therefore path independence of the line integral

$$\int_L d\tilde{\mathbf{G}}^< = \int_L \frac{\partial \tilde{\mathbf{G}}^<}{\partial t_1} dt_1 + \frac{\partial \tilde{\mathbf{G}}^<}{\partial t_2} dt_2 \quad (51)$$

is assured, as required.

Appendix B - Details of the line integration

The tilded Green's function is calculated using the line integral (51) taken along a particular path $(t_{0-}, t_{0+}) \rightarrow (t_1, t_{0+}) \rightarrow (t_1, t_2)$ on the (t_1, t_2) plane:

$$\begin{aligned}\tilde{\mathbf{G}}^<(t_1, t_2) &= \int_L \mathbf{F}^{(1)}(t_1, t_2) dt_1 + \mathbf{F}^{(2)}(t_1, t_2) dt_2 \\ &= \tilde{\mathbf{G}}^<(t_{0-}, t_{0+}) + \int_{t_0}^{t_1} d\bar{t} \mathbf{F}^{(1)}(\bar{t}, t_{0+}) + \int_{t_0}^{t_2} d\bar{t} \mathbf{F}^{(1)}(t_1, \bar{t})\end{aligned}$$

where the matrices $\mathbf{F}^{(1)}$ and $\mathbf{F}^{(2)}$ for both times are given by first derivatives of the tilded Green's function, Eqs. (33) and (34). Here $t_{0-} = t_0 + i0$ is the time t_0 on the upper horizontal part of the contour, while $t_{0+} = t_0 - i0$ is the later time lying on the lower horizontal track of γ . This guarantees the correct time ordering for the lesser function. Next we

use the fact that the Matsubara Green's function provides the boundary conditions for the lesser Green's function at the special point (t_{0-}, t_{0+}) :

$$\tilde{\mathbf{G}}^<(t_{0-}, t_{0+}) = \mathbf{G}^<(t_{0-}, t_{0+}) = \mathbf{G}^M(0, 0^+)$$

This is a way of incorporating information on the system preparation into a description of its dynamics. Hence, one can write:

$$\begin{aligned} \tilde{\mathbf{G}}(t_1, t_2) - \mathbf{G}^M(0, 0^+) &= -i \int_{t_0}^{t_1} d\bar{t} e^{i\mathbf{h}^{eff}(\bar{t}-t_0)} [(\boldsymbol{\Sigma}^< \cdot \mathbf{G}^a) + (\boldsymbol{\Sigma}^\top \star \mathbf{G}^\Gamma)]_{(\bar{t}, t_{0+})} \\ &+ i \int_{t_0}^{t_2} d\bar{t} e^{i\mathbf{h}^{eff}(t_1-t_0)} [(\mathbf{G}^r \cdot \boldsymbol{\Sigma}^<) + (\mathbf{G}^\top \star \boldsymbol{\Sigma}^\Gamma)]_{(t_1, \bar{t})} e^{-i(\mathbf{h}^{eff})^\dagger(\bar{t}-t_0)} \equiv \sum_{i=1}^4 \mathcal{G}^{(i)} \end{aligned} \quad (52)$$

There are four terms here, $\mathcal{G}^{(i)}$ ($i = 1, \dots, 4$), two coming from each integral, and we shall evaluate them one at a time. As some parts of the calculation are similar to the one reported in [8], we only briefly state the main steps here. It is easily seen that the first term $\mathcal{G}^{(1)}$ in the first integral in the right hand side above is zero since

$$(\boldsymbol{\Sigma}^< \cdot \mathbf{G}^a)_{(\bar{t}, t_{0+})} = \int_{t_0}^{\infty} dt' \boldsymbol{\Sigma}^<(\bar{t}, t') \mathbf{G}^a(t', t_{0+})$$

contains the advanced Green's function $\mathbf{G}^a(t', t_0) \propto \theta(t_0 - t')$ for $t' > t_0$. The second term $\mathcal{G}^{(2)}$ in the first integral in Eq. (52) includes the convolution integral $(\boldsymbol{\Sigma}^\top \star \mathbf{G}^\Gamma)_{(\bar{t}, t_0)}$. Using Eq. (24) for the left Green's function, we replace $\mathbf{G}^\Gamma(\tau, t_{0+})$ in the convolution integral $(\boldsymbol{\Sigma}^\top \star \mathbf{G}^\Gamma)_{(\bar{t}, t_{0+})}$ with $\mathbf{G}^M(\tau, 0^+)$. Using Eq. (15) for the left self-energy and expanding the Matsubara Green's function into the Fourier series (20) and integrating over τ , we obtain:

$$(\boldsymbol{\Sigma}^\top \star \mathbf{G}^\Gamma)_{(\bar{t}, t_{0+})} = \left(\sum_{\alpha} \boldsymbol{\Gamma}_{\alpha} e^{-i\psi_{\alpha}(\bar{t}, t_0)} \right) \int \frac{d\omega'}{2\pi} e^{-i\omega'(\bar{t}-t_0)} \frac{i}{\beta} \sum_q \frac{\mathbf{G}^M(\omega_q)}{\omega_q - \omega' + \mu} e^{\omega_q 0^+}$$

The sum over Matsubara frequencies is transformed using the well-known formula

$$\frac{i}{\beta} \sum_q Q(\omega_q) e^{\omega_q 0^+} = \int \frac{d\omega}{2\pi} f(\omega) [Q(\omega^-) - Q(\omega^+)] \quad (53)$$

where $\omega^{\pm} = \omega \pm i0$. Then the ω' -integration is easily performed in the complex plane, and we obtain for the second term in the first integral in Eq. (52):

$$\mathcal{G}^{(2)} = \int \frac{d\omega}{2\pi} f(\omega - \mu) \sum_{\alpha} \mathbf{K}_{\alpha}(t_1; \omega) \boldsymbol{\Gamma}_{\alpha} \mathbf{G}^a(\omega)$$

where the \mathbf{K}_{α} matrix is given by Eq. (36) and we have used the fact, following from the comparison of Eqs. (21) and (29), that $\mathbf{G}^M(\omega^- - \mu) \equiv \mathbf{G}^a(\omega)$.

The third contribution to the line integral coming from the term $(\mathbf{G}^r \cdot \boldsymbol{\Sigma}^<)_{(t_1, \bar{t})}$ in the second integral in Eq. (52) is obtained immediately owing to simple expressions (28) and (14) for the retarded Green's function and the lesser self-energy, respectively:

$$\mathcal{G}^{(3)} = i \int \frac{d\omega}{2\pi} f(\omega - \mu) \sum_{\alpha} \mathbf{K}_{\alpha}(t_1; \omega) \boldsymbol{\Gamma}_{\alpha} \mathbf{K}_{\alpha}^{\dagger}(t_2; \omega)$$

Finally, to calculate the last object $\mathcal{G}^{(4)}$ in the expression (52), one needs the term $(\mathbf{G}^\top \star \boldsymbol{\Sigma}^\Gamma)_{(t_1, \bar{t})}$ which is first manipulated into the expression

$$(\mathbf{G}^\top \star \boldsymbol{\Sigma}^\Gamma)_{(t_1, \bar{t})} = e^{-i\mathbf{h}^{eff}(t_1-t_0)} \left[(\mathbf{G}^M \star \boldsymbol{\Sigma}^\Gamma)_{(0^-, \bar{t})} - i \int_{t_0}^{t_1} d\bar{t}' e^{i\mathbf{h}^{eff}(\bar{t}'-t_0)} (\boldsymbol{\Sigma}^\top \star \mathbf{G}^M \star \boldsymbol{\Sigma}^\Gamma)_{(\bar{t}', \bar{t})} \right] \quad (54)$$

using the formula (23) for the right Green's function. Above, in the second term we have a double convolution integral along the imaginary track. However, it is straightforward to show using explicit expressions (16) and (15) for both self-energies and the expansion (20) for the Matsubara Green's function, that this term is zero:

$$(\boldsymbol{\Sigma}^\top \star \mathbf{G}^M \star \boldsymbol{\Sigma}^\Gamma)_{(\bar{t}', \bar{t})} = \frac{i}{\beta} \sum_q \left(\sum_{\alpha} \boldsymbol{\Gamma}_{\alpha} e^{-i\psi_{\alpha}(\bar{t}', t_0)} \right) \mathbf{G}^M(\omega_q) \left(\sum_{\alpha'} \boldsymbol{\Gamma}_{\alpha'} e^{i\psi_{\alpha'}(\bar{t}, t_0)} \right)$$

$$\times \int \frac{d\omega_1}{2\pi} \frac{e^{-i\omega_1(\bar{t}-t_0)}}{\omega_q - \omega_1 + \mu} \int \frac{d\omega_2}{2\pi} \frac{e^{i\omega_2(\bar{t}-t_0)}}{\omega_q - \omega_2 + \mu}$$

Indeed, the ω_1 integral is only non-vanishing when $Im(\omega_q) < 0$, while the ω_2 integral survives only when $Im(\omega_q) > 0$. We thus need only to calculate the following expression contained in the first term in (54):

$$(\mathbf{G}^M \star \Sigma^\Gamma)_{(0^-, \bar{t})} = \int \frac{d\omega}{2\pi} e^{i\omega(\bar{t}-t_0)} \frac{i}{\beta} \sum_q \frac{\mathbf{G}^M(\omega_q)}{\omega_q - \omega + \mu} e^{\omega_q 0^+} \left(\sum_\alpha \Gamma_\alpha e^{i\psi_\alpha(\bar{t}, t_0)} \right)$$

Once again, we perform the summation over the Matsubara frequencies using formula (53) and then perform the ω integration in the complex plane, leading to the following result for the final contribution to the line integral:

$$\mathcal{G}^{(4)} = - \int \frac{d\omega}{2\pi} f(\omega - \mu) \mathbf{G}^r(\omega) \sum_\alpha \Gamma_\alpha \mathbf{K}_\alpha^\dagger(t_2; \omega)$$

Summing up all four terms, and taking into account that

$$\mathbf{G}^M(0, 0^+) = i \int \frac{d\omega}{2\pi} f(\omega - \mu) \sum_\alpha \mathbf{A}_\alpha(\omega)$$

we obtain the result (38) given in the text.

Appendix C - Exact Expression for the Current Implementation

When one substitutes (47) and (48) into the formula (38), one can separate the resulting formula into three terms, two of which decay due to factors of $e^{-\Gamma(t-t_0)/2}$ and $e^{-\Gamma(t-t_0)}$. These expressions are stated here for completeness:

$$\begin{aligned} I_L^{(1)}(t) &= e^{-\frac{\Gamma}{2}(t-t_0)} 4 \int \frac{d\omega}{2\pi} f(\omega - \mu) \Gamma_L \left[Im \left[e^{i(\omega+V_L-\varepsilon_0)(t-t_0)} e^{i\frac{A_L}{\Omega_L} \sin(\Omega_L t)} \right. \right. \\ &\quad \times \left. \left. \left(\sum_n J_n \left(\frac{A_L}{\Omega_L} \right) G^r(\omega + V_L + n\Omega_L) e^{-in\Omega_L t_0} - G^r(\omega) e^{-i\frac{A_L}{\Omega_L} \sin(\Omega_L t_0)} \right) \right] \right] \\ &\quad + Re \left[\Gamma_L \sum_n J_n \left(\frac{A_L}{\Omega_L} \right) G^a(\omega + V_L + n\Omega_L) e^{i(\omega+V_L-\varepsilon_0)(t-t_0)} e^{in\Omega_L t} \right. \\ &\quad \times \left. \left. \left(\sum_m J_m \left(\frac{A_L}{\Omega_L} \right) G^r(\omega + V_L + m\Omega_L) e^{-im\Omega_L t_0} - G^r(\omega) e^{i\frac{A_L}{\Omega_L} \sin(\Omega_L t_0)} \right) \right] \right] \end{aligned} \quad (55)$$

$$\begin{aligned} I_L^{(2)}(t) &= e^{-\Gamma(t-t_0)} 2 \int \frac{d\omega}{2\pi} f(\omega - \mu) \Gamma_L^2 \left[2Re \left[\sum_n J_n \left(\frac{A_L}{\Omega_L} \right) e^{i\frac{A_L}{\Omega_L} \sin(\Omega_L t_0)} e^{-in\Omega_L t_0} G^r(\omega + V_L + n\Omega_L) G^a(\omega) \right] \right. \\ &\quad \left. - \sum_{n,m} J_n \left(\frac{A_L}{\Omega_L} \right) J_m \left(\frac{A_L}{\Omega_L} \right) G^r(\omega + V_L + n\Omega_L) G^a(\omega + V_L + m\Omega_L) e^{i\Omega_L(m-n)t_0} - G^r(\omega) G^a(\omega) \right] \end{aligned}$$

The long-time behaviour of the current discussed in 3 is therefore given by the remaining term in the current formula:

$$\begin{aligned} \lim_{t_0 \rightarrow -\infty} I_L(t) &= 2 \int \frac{d\omega}{2\pi} f(\omega - \mu) \Gamma_L \left[2Im \left[\sum_n J_n \left(\frac{A_L}{\Omega_L} \right) e^{-i\frac{A_L}{\Omega_L} (\sin(\Omega_L t) - \sin(\Omega_L t_0))} e^{in\Omega_L t} G^a(\omega + V_L + n\Omega_L) \right] \right. \\ &\quad \left. - \sum_{n,m} J_n \left(\frac{A_L}{\Omega_L} \right) J_m \left(\frac{A_L}{\Omega_L} \right) e^{i(m-n)\Omega_L t} G^r(\omega + V_L + n\Omega_L) \Gamma_L G^a(\omega + V_L + m\Omega_L) - G^r(\omega) \Gamma_R G^a(\omega) \right] \end{aligned} \quad (56)$$

References

- [1] T. Matsubara. *Prog. Theor. Phys.*, 14(4):351, 1955.
- [2] Paul C. Martin and Julian Schwinger. *Phys. Rev.*, 115:1342, 1959.
- [3] O. V. Konstantinov and V. I. Perel'. *Sov. Phys. JETP*, 12(1):142, 1961.
- [4] L. P. Kadanoff and G. Baym. *Quantum statistical mechanics: Green's function methods in equilibrium and nonequilibrium problems*. New York: Benjamin, 1962.
- [5] Leonid V. Keldysh. *Sov. Phys. JETP*, 20(4), 1964.
- [6] D. C. Langreth. *Linear and Non-Linear Response Theory with Applications*, volume 17 of *NATO Advanced Studies Series B*, page 3. Plenum, New York/London, 1976.
- [7] J. Rammer and H. Smith. *Rev. Mod. Phys.*, 58:323, 1986.
- [8] G. Stefanucci and R. van Leeuwen. *Nonequilibrium Many-Body Theory of Quantum Systems*. Cambridge University Press, 2013.
- [9] G. Baym and L. P. Kadanoff. *Phys. Rev.*, 124:287, 1961.
- [10] D. L. Klein, R. Roth, A. Lim, P. Alivisatos, and P. L. McEuen. *Nature*, 389(6652):699, 1997.
- [11] R. Landauer. *IBM J. Res. Dev.*, 1(3):223, 1957.
- [12] R. Landauer. *Phil. Mag.*, 21(172):863, 1970.
- [13] M. Büttiker and R. Landauer. *Phys. Rev. Lett.*, 49:1739, 1982.
- [14] M. Büttiker. *Phys. Rev. Lett.*, 65:2901, 1990.
- [15] M. Büttiker. *Phys. Rev. B*, 46:12485, 1992.
- [16] M. Di Ventra and N. D. Lang. *Phys. Rev. B*, 65:045402, 2001.
- [17] M. Di Ventra, S.-G. Kim, S. T. Pantelides, and N. D. Lang. *Phys. Rev. Lett.*, 86:288, 2001.
- [18] J. M. Krans, J. M. Van Ruitenbeek, V. V. Fisun, I. K. Yanson, and L. J. De Jongh. *Nature*, 375(6534):767, 1995.
- [19] N. Agrait, A. L. Yeyati, , and J. M. Van Ruitenbeek. *Phys. Rep.*, 377(2):81, 2003.
- [20] L. Venkataraman, J. E. Klare, C. Nuckolls, M. S. Hybertsen, and M. L. Steigerwald. *Nature*, 442(7105):904, 2006.
- [21] Y. M. Blanter and Büttiker. *M. Phys. Rep.*, 336(1):1, 2000.
- [22] P. J. Burke. *Solid State Electron.*, 48:1981, 2004.
- [23] S. D. Li, Z. Yu, S.-F. Yen, W. C. Tang, and P. J. Burke. *Nano. Lett.*, 4(4):753, 2004.
- [24] Y. M. Lin, K. A. Jenkins, A. Valdes-Garcia, J. P. Small, D. B. Farmer, and P. Avouris. *Nano. Lett.*, 9(1):422, 2009.
- [25] M. Moskalets. *Scattering Matrix Approach to Non-Stationary Quantum Transport*. Imperial College Press, 2012.
- [26] C. Caroli, R. Combescot, P. Nozieres, and D. Saint-James. *J. Phys. C: Solid State Phys.*, 4(8):916, 1971.
- [27] C. Caroli, R. Combescot, D. Lederer, P. Nozieres, and D. Saint-James. *J. Phys C: Solid State Phys.*, 4(16):2598, 1971.
- [28] N. S. Wingreen, A.-P. Jauho, and Y. Meir. *Phys. Rev. B*, 48:8487, Sep 1993.
- [29] A.-P. Jauho, N. S. Wingreen, and Y. Meir. *Phys. Rev. B*, 50:5528, 1994.
- [30] M. Di Ventra. *Electrical transport in nanoscale systems*. Cambridge University Press, 2008.
- [31] M. Cini. *Phys. Rev. B*, 22:5887, 1980.
- [32] G. Stefanucci and C.-O. Almbladh. *Phys. Rev. B*, 69:195318, 2004.
- [33] R. Tuovinen, E. Perfetto, G. Stefanucci, and R. van Leeuwen. *Phys. Rev. B*, 89:085131, 2014.

- [34] Riku Tuovinen, Robert van Leeuwen, Enrico Perfetto, and Gianluca Stefanucci. *J. Phys.: Conf. Ser.*, 427:012014, 2013.
- [35] N. E. Dahlen, R. van Leeuwen, and A. Stan. 35(1):324, 2006.
- [36] R. van Leeuwen, N. E. Dahlen, G. Stefanucci, C.-O. Almbladh, and U. von Barth. *Time-Dependent Density Functional Theory*, chapter Introduction to the Keldysh Formalism. Springer, 2006.
- [37] P. Myöhänen, A. Stan, G. Stefanucci, and R. van Leeuwen. *Phys. Rev. B*, 80:115107, 2009.
- [38] S.-H. Ke, R. Liu, W. Yang, and H. U. Baranger. *J. Chem. Phys.*, 132(23), 2010.
- [39] D. C. Langreth and J. W. Wilkins. *Phys. Rev. B*, 6(9):3189, 1972.
- [40] M. Ridley, A. MacKinnon, and L. Kantorovich. in preparation.
- [41] P. Danielewicz. *Ann. Phys.*, 152:239, 1984.
- [42] A. Kartsev, C. Verdozzi, and G. Stefanucci. *Eur. Phys. J. B*, 87(1):1, 2014.
- [43] S. Latini, E. Perfetto, A.-M. Uimonen, R. van Leeuwen, and G. Stefanucci. *Phys. Rev. B*, 89:075306, 2014.
- [44] Y. Imry and R. Landauer. *Rev. Mod. Phys.*, 71:S306, 1999.
- [45] M. Di Ventra, S. T. Pantelides, and N. D. Lang. *Phys. Rev. Lett.*, 84:979, 2000.
- [46] S. Kohler, J. Lehmann, and P. Hänggi. *Physics Reports*, 406(6):379, 2006.